SAND REPORT
SAND2003-2336
Unlimited Release
Printed July 2003

An Approach to Model Validation and Model-Based Prediction Polyurethane Foam Case Study

Brian M. Rutherford, Kevin J. Dowding

Prepared by
Sandia National Laboratories
Albuquerque, New Mexico 87185 and Livermore, California 94550

Sandia is a multiprogram laboratory operated by Sandia Corporation, a Lockheed Martin Company, for the United States Department of Energy under Contract DE-AC04-94AL85000.

Issued by Sandia National Laboratories, operated for the United States Department of Energy by Sandia Corporation.

Available to DOE and DOE contractors from
U.S. Department of Energy
Office of Scientific and Technical Information
P.O. Box 62
Oak Ridge, TN 37831

Telephone: (865)576-8401
Facsimile: (865)576-5728
E-Mail: reports@adonis.osti.gov
Online ordering: http://www.doe.gov/bridge

Available to the public from
U.S. Department of Commerce
National Technical Information Service
5285 Port Royal Rd
Springfield, VA 22161

Telephone: (800)553-6847
Facsimile: (703)605-6900
E-Mail: orders@ntis.fedworld.gov
Online order: http://www.ntis.gov/ordering.htm

SAND2003-2336
Unlimited Release
Printed July 2003

An Approach to Model Validation and Model-Based Prediction -- Polyurethane Foam Case Study

Brian M. Rutherford
Independent Surveillance Assessment
and Statistics Department

Kevin J. Dowding
Validation and Uncertainty Quantification Department

Sandia National Laboratories
P.O. Box 5800
Albuquerque, NM 87185-0829

Abstract

Enhanced software methodology and improved computing hardware have advanced the state of simulation technology to a point where large physics-based codes can be a major contributor in many systems analyses. This shift toward the use of computational methods has brought with it new research challenges in a number of areas including characterization of uncertainty, model validation, and the analysis of computer output. It is these challenges that have motivated the work described in this report.

Approaches to and methods for model validation and (model-based) prediction have been developed recently in the engineering, mathematics and statistical literatures. In this report we have provided a fairly detailed account of one approach to model validation and prediction applied to an analysis investigating thermal decomposition of polyurethane foam. A model simulates the evolution of the foam in a high temperature environment as it transforms from a solid to a gas phase. The available modeling and experimental results serve as data for a case study focusing our model validation and prediction developmental efforts on this specific thermal application.

We discuss several elements of the "philosophy" behind the validation and prediction approach:

- We view the validation process as an activity applying to the use of a specific computational model for a specific application. We do acknowledge, however, that an important part of the overall development of a computational simulation initiative is the feedback provided to model developers and analysts associated with the application.
- We utilize information obtained for the calibration of model parameters to estimate the parameters and quantify uncertainty in the estimates. We rely, however, on validation data (or data from similar analyses) to measure the variability that contributes to the uncertainty in predictions for specific systems or units (unit-to-unit variability).
- We perform statistical analyses and hypothesis tests as a part of the validation step to provide feedback to analysts and modelers. Decisions on how to proceed in making model-based predictions are made based on these analyses together with the application requirements. Updating modifying and understanding the boundaries associated with the model are also assisted through this feedback.
- We include a "model supplement term" when model problems are indicated. This term provides a (bias) correction to the model so that it will better match the experimental results and more accurately account for uncertainty. Presumably, as the models continue to develop and are used for future applications, the causes for these apparent biases will be identified and the need for this supplementary modeling will diminish.
- We use a response-modeling approach for our predictions that allows for general types of prediction and for assessment of prediction uncertainty.

This approach is demonstrated through a case study supporting the assessment of a weapons response when subjected to a hydrocarbon fuel fire. The foam decomposition model provides an important element of the response of a weapon system in this abnormal thermal environment. Rigid foam is used to encapsulate critical components in the weapon system providing the needed mechanical support as well as thermal isolation. Because the foam begins to decompose at temperatures above 250° C, modeling the decomposition is critical to assessing a weapons response.

In the validation analysis it is indicated that the model tends to "exaggerate" the effect of temperature changes when compared to the experimental results. The data, however, are too few and to restricted in terms of experimental design to make confident statements regarding modeling problems. For illustration, we assume these indications are correct and compensate for this apparent bias by constructing a model supplement term for use in the model-based predictions. Several hypothetical prediction problems are created and addressed. Hypothetical problems are used because no guidance was provided concerning what was needed for this aspect of the analysis. The resulting predictions and corresponding uncertainty assessment demonstrate the flexibility of this approach.

TABLE OF CONTENTS

List of Figures

List of Tables

This Page Intentionally Left Blank

I. Introduction

The ability to make credible system assessments, predictions and design decisions related to engineered systems and other complex phenomenon is key to a successful program for systems analysis within the DOE Complex and elsewhere. Historically, these assessments have been based, to a large extent, on results from physical tests at both the component and system level. Recently, many of these large-scale analyses have turned to computational simulation to provide increased support. The evolution of software methodology and of improved computing hardware has advanced the state of simulation technology to a point where computational simulation can provide important information efficiently for these analyses. These changes, however, have brought with them new challenges in a number of areas including characterization of uncertainty, model validation, and to the analysis of computational results. It is these challenges that have motivated the work described in this report.

The Validation Metrics Project (VMP) is one of several projects at Sandia National Laboratories supported through the Accelerated Strategic Computing Initiative (ASCI) to address these challenges. The work described in this report was supported through the ASCI VMP. We present the methods used and results obtained in a polyurethane foam thermal decomposition case study involving model calibration, model validation and model-based prediction. The primary purpose of the report is to present one view of the model validation process and to discuss how it relates to other methods used in the current literature of this rapidly developing area of research.

The application selected for this demonstration involves the rate of thermal decomposition of polyurethane foam. In a weapon system, rigid foam is used to encapsulate critical components. The foam provides needed mechanical support, but also thermal isolation. In an abnormal environment, such as a hydrocarbon fuel fire, the rigid foam will decompose when the temperature exceeds 250 C and expose critical components to the harsh thermal environment. Historically, based on a single test, radiation parameters in weapon models have been "tuned" to reflect the protective effect of foam. More recently experiments were conducted and comparisons with existing weapon models discussed in Dobranich and Gill, (1999) have shown that this approach is not adequate for predictive models, thus suggesting that physics-based models are needed for foam decomposition in an abnormal thermal environment. Subsequently, a model has been under development (Hobbs *et al*., 2002) and a program has been initiated to validate this foam decomposition model.

In this report, we provide details for application of one approach to model validation and prediction and discuss several elements of the "philosophy" behind the approach:

- We view the validation process as an activity applying to the use of a specific computational model for a specific application. We do acknowledge, however, that an important part of the overall development of a computational simulation initiative is the feedback provided to model developers and analysts associated with the application.

- We utilize information obtained for the calibration of model parameters to estimate the parameters and quantify uncertainty in the estimates. We rely, however, on validation data (or data from similar analyses) to measure the variability that contributes to the uncertainty in predictions for specific systems or units (unit-to-unit variability).
- We perform statistical analyses and hypothesis tests as a part of the validation step to provide feedback to analysts and modelers. Decisions on how to proceed in making model-based predictions are made based on these analyses together with the application requirements. Updating modifying and understanding the boundaries associated with the model are also assisted through this feedback.
- We include a "model supplement term" when model problems are indicated. This term provides a (bias) correction to the model so that it will better match the experimental results and more accurately account for uncertainty. Presumably, as the models continue to develop and are used for future applications, the causes for these apparent biases will be identified and the need for this supplementary modeling will diminish.
- We use a response-modeling approach for our predictions that allows for general types of prediction and for assessment of prediction uncertainty.

The remainder of this report contains eight sections. In Section II we review some of the tasks involved in a computational analysis. The applications requirements and their interactions with the model validation process are also discussed. Section III describes a mathematical framework that can be used to address model validation and model-based prediction for this application. The framework is not as extensive as several alternatives (referenced later) that are formulated for more general applications, but appears sufficient for our treatment of this case study. Section IV briefly describes the experiments contributing to the application and the data available for the case study. These data include results from two separate sets of experiments involving polyurethane foam -- one set is used for calibration of the model parameters, and the second set for model validation. The focus here is on the validation data. Section V provides a brief discussion of the computational models involved. Details are provided through the references. The next three sections address respectively; calibration, model validation, and model-based prediction. The philosophy behind the approach is described and details are presented on the methods used and results obtained. The report is concluded with a summary section.

An appendix is included to provide further details concerning some of the more technical parts of the analysis. Sections are included for: transformation and propagation of the calibration results, the statistical tests involved in model validation and the response modeling used in prediction. There are a number of occasions throughout the report where we state a general result that we consider to be an important general assertion or conclusion. These results are underlined.

II. The Computational Modeling Process

General

The design and implementation of a flexible and effective model validation and model-based prediction process is a topic of current research and development in areas of (among others) engineering, statistics and mathematics. Recent literature includes a number of papers proposing a common framework for a model validation process and introducing techniques for comparing model-predicted responses to experimental data and for using the models in further prediction. Several of these papers are referenced in this report.

Validation of a computer model for a given application in defined in the U. S. DOE Defense Programs (DOE/DP) ASCI Program Plan (2000) as:

> **Validation** – The process of determining the degree to which a computer model is an accurate representation of the real world from the perspective of the intended model applications.

This definition suggests two important aspects of model validation. First, it is application-driven and, consequently, closely tied to requirements of a specific computational-modeling project. We discuss validation as a process addressing the application requirements. For this case study analysis, some of the requirements and performance criteria used here are hypothetical, because the majority of the experimental work reported here was performed for reasons other than the case study. The requirements and performance criteria were selected to support this demonstration and discussion of validation methodology. We make it clear where we have used hypothetical requirements.

Second, model validation is a process with a number of interacting, related technical tasks. The process we discuss and illustrate in this report is, perhaps, slightly broader in scope than that suggested in the validation definition above, as we address these interrelated technical tasks in some detail. The following subsections are included to address the interactions between requirements and modeling and the validation and prediction process as well as interactions among the individual tasks of the validation process. Figure 1 gives a diagram of the process described here. It is referenced throughout the discussions of this section.

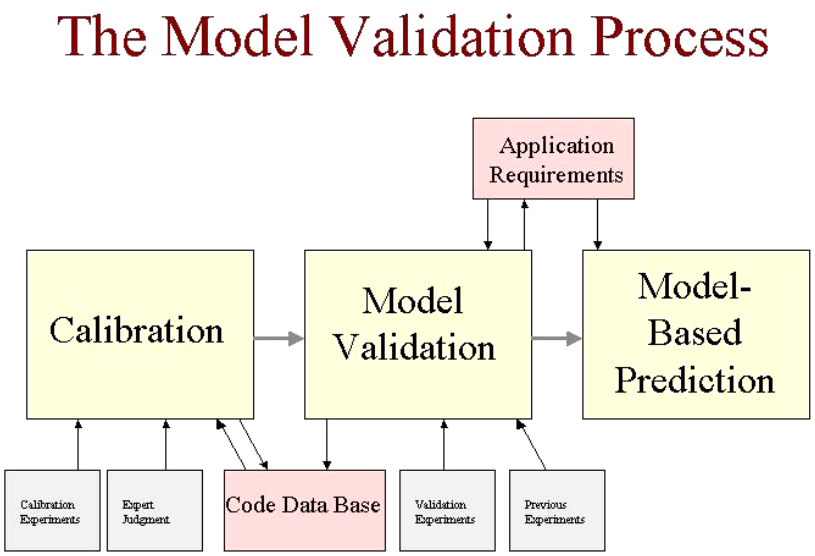

Figure 1. Simple Diagram of the Model Validation Process and its Interactions.

Interaction with Application Requirements

Model validation is a process that can be viewed as an essential component of performing a computational analysis (using a specific code for a specific application). The application requirements dictate what predictive capabilities are needed to address the application objectives and how well the code must perform to be useful in the analysis. The role of the validation process and specifically of the validation experiments within this framework is discussed in detail in Trucano, et al., (2002). The basic relationships are established through Figure 1.2 and the corresponding discussion in that report. The discussion below centers on three aspects of the relationship between application requirements and the model validation process: 1) application requirements determine the responses of interest; 2) application requirements determine the level of agreement needed between computational predictions and experimental results in order to use the model for further prediction; and 3) application requirements specify the predictions required for the application beyond those used in model validation. These aspects are discussed further in the paragraphs that follow.

A question related to (1) above is: What characteristics of system performance (referred to as the "response" in this report) should be evaluated when comparing computational and experimental results? The analysis objectives specified through application requirements should provide the guidelines for the selection of these characteristics. Most applications will involve a large number of measured responses from both the physical experiments and the computational analyses; however, specific functions of these responses may focus on the requirements. For the present case study, foam

decomposition front location as a function of time, and thermal profiles as a function of location and time, are available from both the computational and experimental analyses. However, some of the major concerns related to a weapon in a fire can be addressed by knowing that the model accurately predicts the velocity of the foam thermal decomposition front. In this report, we focus on the velocity data. The lack of specific application objectives for this case study provides some freedom of selection. Our justification is that velocity is a representative characteristic of the front location data and that the relative simplicity associated with the velocity data permits a more clear presentation of the validation issues.

A second aspect of the requirements ((2) above) involves several concepts about which there is little consensus in the recent literature. Several approaches to model-based prediction include provisions for "adjusting" model predictions at points (inputs) where no experimental results are available. Kennedy and O'Hagan, (2001) and Bayarre et al., (2002) provide recent examples where "model inadequacy", the apparent bias in the predicted response for specified inputs, is modeled using a random function model, defined throughout the input space. This practice of supplemental modeling for the predictions based on comparison with experimental results is not a procedure adopted by all proposed approaches to model validation. Some authors suggest testing model results against experimental results and then using the unadjusted model for further predictions required in the analysis if it performs "well enough" in these tests. Others suggest abandoning the model completely if substantial biases are detected. We take the first "model supplement" approach, where we adjust predictions to accommodate discrepancies with experimental data in the appropriate regions of the input space.

A third point of interaction between the application requirements and the validation process ((3) above) is more involved with model-based prediction. The objectives of the analysis will often dictate specific predictions required of the model. These predictions are often outside the range of the validation experiments. We refer to the "prediction space" as that subset of the responses corresponding to inputs where predictions will ultimately be required. We refer to the "application" or "validation space" as that subset of the responses corresponding to the input space from which the model validation experiments were selected. Each space is a subspace of the input region under consideration. See Trucano et al., (2001), Figure 3 and the related discussion, for further description. Another point concerning the required predictions is that they need not be "point" predictions where a predicted response is required for a specified set of inputs. Averages over a range of inputs, probabilities associated with specific events such as responses exceeding a threshold response (reliability analyses, for instance) or worst-case response are examples of more involved prediction requirements. We address hypothetical prediction requirements in Section VIII to demonstrate the flexibility of the approach.

Interaction with the Model Development Effort

It was mentioned in the introduction that we view the Computational Initiative at DOE as an ongoing, constantly improving process. Clearly, however, the models will be used in systems analyses before they reach the level of accuracy that is ultimately desired (if that is ever achieved). To facilitate the improvement process, we would expect information from the statistical tests, performed as a part of the validation effort, to be provided to developers. This information should include limitations and/or boundaries in model performance as well as statistical evidence of overall code performance. In addition, the application will provide model parameter information that might be useful in subsequent applications of the same model. This information should be retained by the developers and integrated with information form other sources to update the distributional assumptions associated with the parameter estimates. In Figure 1, the feedback arrows from the calibration and validation steps to the "Code Data Base" indicate the flow of this information. The distribution of code parameters accumulated from previous applications is one of several inputs to the calibration step as indicated by the arrows in Figure 1.

Elements of the Computational Modeling & Prediction Process

Relationships involved in the validation process between the roles of (input) variable screening and sensitivity analysis, model calibration, model validation, and model-based prediction, are discussed in detail in several of the references; see Kennedy and O'Hagan, (2001), Bayarrie et al., (2002) and Rutherford, et al. (2003). We discuss these elements of the process briefly below.

Sensitivity Analysis

Variable screening and sensitivity analysis are concerned with focusing the analysis on those inputs that have the greatest effect on responses of interest. Most applications will contain a large number of inputs. Tens or even hundreds of inputs are not unlikely. At present, most analyses are constrained in terms of resources (both experimental and computational) and consequently must focus on those inputs that have a relatively large effect on the responses of interest for validation purposes. Variable screening refers to the process of eliminating from further consideration those inputs that don't significantly affect the response. Sensitivity analysis is concerned with estimating the effects of the remaining inputs on the response. In the literature, sensitivity analysis often encompasses the screening process. The polyurethane foam case study includes the inputs: temperature, heating orientation and presence or absence of a component embedded in the foam. Because we start with so few inputs, no special screening experiments are performed: the validation data are used to assess the variables of interest.

Model Calibration

Model calibration involves estimation and statistical modeling of parameters of the mathematical model through comparison with experimental results or through other sources of relevant information. The screening, sensitivity and calibration processes are likely to utilize information from other applications of the code, but may involve application-specific experimentation as well. For the polyurethane foam case study, variable screening and sensitivity analyses were based on the benchmark experiments (described later) validation data. Results of the TGA experiments (also described later) were used to calibrate some of the modeling parameters. Calibration information for the remaining parameters was provided through expert judgment.

Model Validation

We treat model validation as the task of comparing model predictions with experimental results for the purposes of determining whether or not the code is appropriate for the application and determining if a model supplement function might be useful, in supporting the code for further predictions. The approach suggested and used here is to test the model for significant deviations from the experimental results, but then use the model (with a bias correction, if necessary) unless the results indicate unacceptable differences from the measured result (as determined through the application requirements). The purposes in testing the model are to provide feedback to developers on code performance and to identify situations (inputs) for which model performance is unacceptable or in need of additional model development. The purpose of proceeding with the analysis (using an adjusted model, if necessary) is that many models will predict with a bias through a part of the input space (since they are a simplification of reality), but can still be useful in prediction and in providing bounds on the uncertainty in these predictions. The supplemental models can be used to correct apparent model biases. It should be noted that this model supplement is not viewed as a permanent part of the modeling process but rather as a temporary adjustment for specific inputs to compensate for apparent deficiencies in the model over part of the input region. In the polyurethane foam case study, we find that the model appears to predict high velocities for higher temperature results and low velocities for lower temperature results (relative to the 750 C responses). Consequently, a model supplement term is included for further predictions.

Model-Based Prediction

We refer to "model-based prediction" as the task of utilizing the model (after model validation is complete) to make further predictions addressing the application requirements. We illustrate this process for this polyurethane foam case study by considering four separate hypothetical prediction problems. The problems are hypothetical because no specific application requirements were established for this case study. They were selected to illustrate the capabilities of this approach to model validation and model-based prediction.

This Page Intentionally Left Blank

III. Mathematical Framework

General

The recent literature in engineering, statistics, and mathematics provides a number of different approaches to generating a mathematical framework that is general enough to accommodate the model validation process for a wide range of applications. For the present application, some of the detail required for these more general approaches is not needed. In this section we discuss a framework useful for this case study from both the experimental side and the computational side and we develop some of the statistics used for model validation and prediction.

Expressions for the Experimental Results

We consider response values for the application that we are attempting to model to be given by

$$y(\mathbf{x}) = \mu_y(\mathbf{x}) + \varepsilon(\mathbf{x}) \tag{1}$$

where $y(\mathbf{x})$ is the response, **x** represents the input vector of initial and boundary conditions, material properties etc, $\mu_y(\mathbf{x})$ represents the average response for inputs **x** and $\varepsilon(\mathbf{x})$ models deviations from $\mu_y(\mathbf{x})$. For this analysis, *y* in the above expression represents the velocity of the decomposition front averaged over the range from 1 to 2 cm. and the inputs **x** include boundary temperature, heating orientation (experimental geometry), and the presence or absence of an internal component. In cases (like this case study) where predictions are for "units" (e.g., different foam cylinders as were tested in the benchmark experiments), $\mu_y(\mathbf{x})$ is appropriately viewed as an expected result in a statistical sense where the expectation is taken with respect to the "population" of units satisfying the conditions described through **x**.

The term $\varepsilon(\mathbf{x})$ represents the differences in response from $\mu_y(\mathbf{x})$; $\varepsilon(\mathbf{x})$ is a random term with expected value 0 (because of the way $\mu_y(\mathbf{x})$ is defined) and unknown variance $\sigma_y^2(\mathbf{x})$. We refer to σ_y^2 as the unit-to-unit variance. If repeated, tests are performed for a fixed **x**, then an estimate can be provided, say $\hat{\sigma}_y^2(\mathbf{x})$. In this report we do not address the issues related to measurement errors but assume that $\varepsilon(\mathbf{x})$ represents actual differences in unit response compared to their mean value $\mu_y(\mathbf{x})$. A discussion of the possible effects of measurement error in general and specifically for those involved in this case study is given in Dowding et al., (2003). Expression (1) is used here as a statistical model for the experimental response.

Expressions for the Computational Predictions

In pursuing this application through computational analysis, our ultimate goal is to utilize the computational models and construct related terms (mathematical models), if necessary, that can be used in place of expression (1) to make predictions where data aren't available. Experimental estimates for the terms in expression (1) are available for very few values of $\mathbf{x}$. The important aspects of the modeling effort are that predictions can match $\mu_y(\mathbf{x})$ reasonably well in obtaining the expected results and that they can provide a measure of uncertainty in that predicted result that includes the unit-to-unit variability (indicted in expression (1)) together with any further uncertainty generated through the modeling effort. A simple expression that we use to accomplish these goals is given by:

$$p(\mathbf{x}) = m(\mathbf{x},\theta) + \eta(\mathbf{x}) + e(\mathbf{x}) \qquad (2)$$

where: $p(\mathbf{x})$ indicates a "point" prediction for inputs $\mathbf{x}$, $m(\mathbf{x},\theta)$ is the model prediction, $\eta(\mathbf{x})$ is a supplemental mathematical modeling term that may be required if the model appears to yield biased predictions for some $\mathbf{x}$ and $e(\mathbf{x})$ is an estimate for $\varepsilon(\mathbf{x})$. Each of these terms is a random variable for fixed $\mathbf{x}$ and a random field when viewed as a function of the inputs $\mathbf{x}$. The three terms on the right are discussed in more detail below.

Model Specification

Note, that in the model specification, we make a distinction between the inputs $\mathbf{x}$ and the code parameters θ. The inputs $\mathbf{x}$ appear in both the physical (experimental) and modeling expressions ((1) and (2)). The components of $\mathbf{x}$ represent initial and boundary conditions or important factors or variables that may affect the responses. Ranges of interest for the inputs $\mathbf{x}$ are specified for the application through the application requirements. Code parameters, θ, provide inputs to the simulations only. The parameters of interest here are those that specify unknown quantities essential to the physics that are not necessarily calculated or measured, or even necessarily meaningful on the experimental side. These parameters are often modeled using a probability distribution. For these cases, we use the notation $F(\theta)$ for the distribution function and $f(\theta)$ for the density function. More detail on the model parameters θ are given in Section VI.

Model Supplement Function

The model supplementary term $\eta(\mathbf{x})$ and its variance are based on differences between experimental and model results in the validation. In the Model Validation Section, we perform statistical tests to see if comparing experimental results to model predictions suggests the use of $\eta(\mathbf{x})$. For the present application we use the transformed differences:

$$d^*(\mathbf{x}) = \ln(y(\mathbf{x})/p(\mathbf{x})) \qquad \text{(where ln(.) is the natural logarithm)}$$

because the transformed results better satisfy the assumptions of the tests used. In the Model-Based Prediction Section, we use the actual differences:

$$d(\mathbf{x}) = (y(\mathbf{x}) - p(\mathbf{x}))$$

for constructing the term $\eta(\mathbf{x})$.

Unit-to-Unit Differences

The unit-to-unit variability captured through $e(\mathbf{x})$ (or $\varepsilon(\mathbf{x})$) is estimated directly from comparison of the results from the validation experiments. For k data values at fixed $\mathbf{x}$ (say $\mathbf{x}'$), we estimate the unit-to-unit (sampling) variability using

$$\hat{\sigma}_y^2(\mathbf{x}') = \frac{1}{k-1}\sum_{i=1}^{k}\left(y_i(\mathbf{x}') - \bar{y}(\mathbf{x}')\right)^2$$

where $y_i(\mathbf{x}'),\ i = 1,\ldots,k$ are the k responses and $\bar{y}(\mathbf{x}')$ is their average. If it is reasonable to assume a constant variance, not dependent on the inputs, we use the notation $\hat{\sigma}_y^2$ without the argument $\mathbf{x}$. The estimated uncertainty in the mean response is given by the variance $\hat{\sigma}_{\mu_y}^2(\mathbf{x}') = \hat{\sigma}_y^2(\mathbf{x}')/k$. Note that additional testing using inputs $\mathbf{x}'$ will reduce this uncertainty.

This Page Intentionally Left Blank

IV. Supporting Experiments and Experimental Results

General

Two sets of experiments were utilized in this case study – The TGA experiments and the benchmark experiments. The TGA data were used for model calibration only. See (Dowding, et. al, 2003) for a description of these experiments and their results. In this section we provide a brief description of the benchmark experiments conducted and used for this case study. We begin with an overview of the experimental design and then give details of the experimental setup and procedures.

Experimental Design

Nine experiments, run at ambient pressure that included different configurations, orientations, and thermal boundary conditions are given in Table 1, (from Dowding, et. al, (2003)). Table 1 summarizes the experimental design and gives the velocity results.

Table 1. Experimental Design for the Benchmark Experiments

Experiment No.	Density (lb/ft^3)	Cup Plate Temperature	Orientation of Cup Plate	Component	Velocity (cm/min)
1	22.7	600 C	Bottom	None	0.1307
2	22.7	750 C	Bottom	None	0.2323
5	22.7	750 C	Bottom	Stainless Steel	0.1958
10	22.7	750 C	Top	None	0.2110
11	22.7	750 C	Side	None	0.2582
13	22.7	750 C	Side	None	0.2154
14	22.7	900 C	Bottom	None	0.3483
15	22.7	750 C	Bottom	Aluminum	0.2755
16	22.7	1000 C	Bottom	Stainless Steel	0.5578

The experimental design consists of a base case experiment 750 C/Bottom/None and a series of experiments changing one of these "factors" at a time from the base case. The single exception is experiment 16 where both temperature and internal component were changed. Replicated experiments, 11 and 13, were performed at conditions 750 C/Side/None.

Experimental Setup

A schematic diagram of the experimental setup is shown in Figure 2. All the experiments included a polyurethane foam cylinder partially contained in a thin walled stainless steel sample cup. The foam cylinder was 8.8 cm in diameter and 14.6 cm long. The stainless steel cup consisted of a 0.5 mm thick walled cylinder 7.3 cm long with a 6 mm thick disk

press fit at one end. The inside diameter was closely matched to the foam cylinder. For some of the experiments, a solid stainless steel cylinder or hollow aluminum cylinder was embedded within the polyurethane foam to simulate a protected component. Heating of the foam was accomplished with an array of heat lamps. The relatively thick cup base resulted in uniform heating of the foam. Thermocouple measurements provide the temperature at boundaries, which are needed for the model heat transfer calculations.

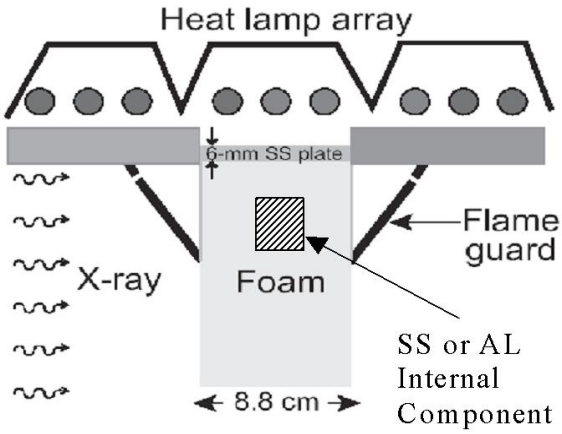

Figure 2. Schematic diagram of foam heating apparatus in "top" configuration (Hobbs et. al, 2002).

The approximate locations of the vent holes and the thermocouples are shown in Figure 3. Representative time history traces of temperature are also shown. The top three curves labeled '0' are for the 6 mm stainless steel plate (cup base). The remaining six traces are the sidewall plate temperatures for the 600 C experiment.

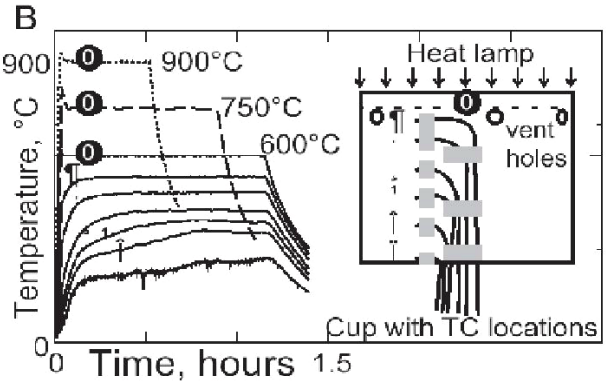

Figure 3. Representative temperature history used as boundary conditions in the model results. Vent holes and thermocouple locations are also shown. (Hobbs et al., 2002).

In addition to the temperature measurements made using the thermocouples shown in Figure 3, X-rays were used to track the front location of the decomposing polyurethane.

An example of the X-ray images from experiment number 2 is shown in Figure 4. The images show that the front has receded 1.1, 2.4 and 4.0 cm.

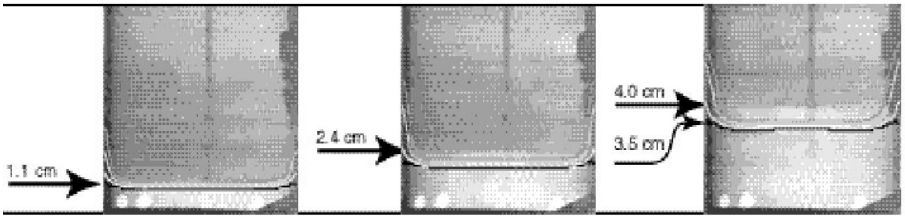

Figure 4. X-ray images of front location of decomposing foam front. Model results are overlaid on the X-ray (Hobbs et al., 2002).

For validation purposes, a quantitative comparison of the experimental results with the model prediction is needed. To obtain quantitative information the X-ray images were digitized and the location of the decomposing front was tracked. Distance from the heated plate to the front provides a quantitative measure of the experiment that can be extracted from the X-ray. Front location as a function of time data taken from time-resolved images are shown in Figure 5. Velocity data, listed in the last column of Table 1, are calculated using the time that it takes the front location to travel from 1 cm to 2 cm.

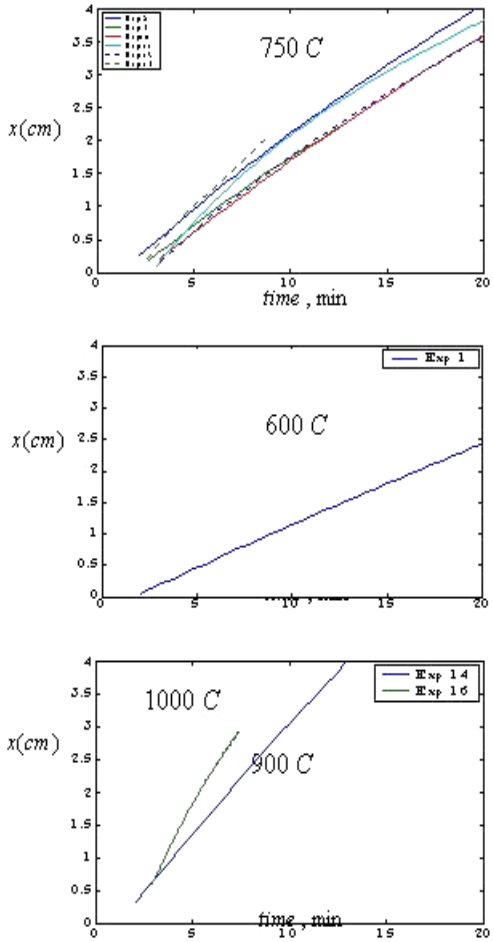

Figure 5. Validation data from the benchmark experiments.

This Page Intentionally Left Blank

V. Computational Models

General

In this section we provide a brief description of the computational code used for this case study and the parameters used in association with it. We begin by describing how and why the COYOTE code was selected and then give details of the model setup and parameters used.

Computational Code

Model results for the benchmark experiments come from the thermal analysis code COYOTE, Gartling, et al., (1994). Although the intent of this study was to validate the application of Calore, and all verification has addressed Calore, Bova et al. (2002) not all modeling capabilities had been implement in Calore with sufficient time to meet our schedule. Applying COYOTE in the validation study is relevant to understanding the accuracy of Calore because we are validating the mathematical models and algorithms that are executed when applying the code to the specified application. Since the mathematical model and algorithms in COYOTE are essentially identical to those in Calore, assessing the accuracy of COYOTE is indicative of the accuracy of Calore (for this application).

Computational Setup and Model Parameters

The mesh used in the model for the benchmark experiments is shown in Figure 6. Radial symmetry is assumed. The model has at least four material regions: reactive foam, non-reactive foam, 304 stainless steel heated plate, and 321 stainless can. In some cases a fifth material region, either 304 stainless steel or 6061 aluminum, is added when an internal component is included (a stainless steel slug is shown in Figure 6). The reactive foam will have chemical reactions (if temperature is sufficiently high), while the non-reactive foam will not have chemical reactions. Defining a block as non-reactive foam saves computations by not having to solve the chemical equations over the region that we know (from experimental data) will not reach temperatures to sustain chemical reaction. The thermophysical properties are the same for reactive and non-reactive foam.

Boundary conditions for the model are taken from the experimental measurements (Figure 3). A thermocouple located within the heated plate provides the transient temperature imposed as a boundary condition along the heated surface, $T_p(t)$. Thermocouples along the outer surface of the can are use to impose the transient temperature along the outer surface of the can, $T_c(x,t)$. Elements that are located between thermocouple locations are assigned values through interpolation.

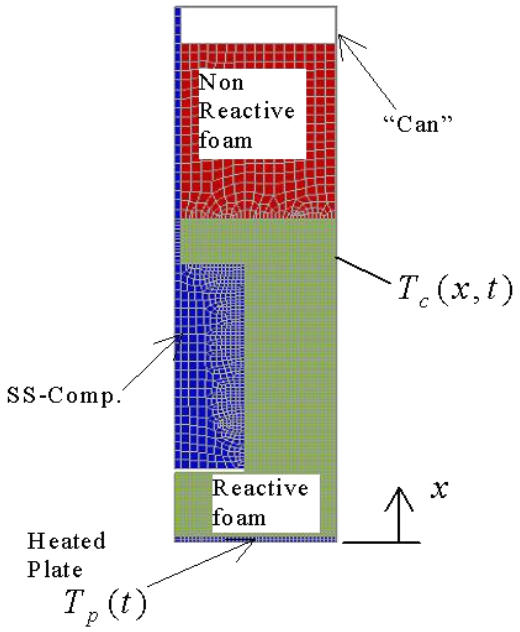

Figure 6. Mesh for benchmark model results.

The mathematical model is coupled thermal diffusion, chemical kinetics, and enclosure radiation (after the reactive foam has decomposed and opens a void between the heated plate and surface of the foam); see Dowding et. al. (2003) for a complete description of the mathematical model. We use model parameters (the θ) for chemical kinetics, (foam) decomposition and radiation parameters. Values for these parameters are listed in Tables 2 through 5. Activation energies for the foam, estimated from the TGA experiments, are provided in Table 2. Additional parameters are needed for the foam: initial bond population, density, heat of reaction, emissivity, degree of monomer and element death. These are given in Table 3. Thermophysical properties of the foam, up to 523 K (onset of decomposition) are listed in Table 4; beyond this temperature, values are obtained through extrapolation. All grades of stainless steel use the thermophysical properties listed in Table 5. The parameter values listed in Tables 1 through 5 give the parameter estimates. Twenty five of these (those in Tables 2 and 3) were assigned probability distributions. Details are given in Section V1.

Table 2. Estimated Activation Energies

Parameters	Mean	Variance
E1 (activation energy)	50209	$(238.8)^2$
E2	50567	$(199.0)^2$
E3	49374	$(107.3)^2$
E4	50408	$(151.6)^2$
E5	49985	$(131.0)^2$
E6	49508	$(211.0)^2$
E7	50397	$(78.36)^2$
E8	49276	$(110.3)^2$
E9	51513	$(127.6)^2$
E10	49791	$(132.7)^2$
E11	50195	$(141.4)^2$
E12	50147	$(269.8)^2$
E13	50201	$(137.8)^2$
E14	51081	$(209.3)^2$
E15	49608	$(168.6)^2$
E16	49730	$(79.01)^2$
E_dist (distribution parameter)	3521.4	$(16.35)^2$

Table 3. Model Parameters*

Parameters	Mean	Variance
initial temp	300	$(3)^2$
initial bond population (l_0)	0.78	$(0.05)^2$
Density (ρ)	0.364	$(0.0364)^2$
specific heat (c)	1	$(0.1)^2$
heat of reaction (h_r)	20.6	$(2.06)^2$
Emissivity (ε)	0.8	$(0.05)^2$
σ+1	2.8	$(.28)^2$
death criteria (k_e)	0.036	$(.0069)^2$

* *Thermal conductivity is not included in this list because it was used as a discretization bias corrector (Hobbs et al., 2002). For an idea of the relative importance of thermal conductivity see Hobbs, et al. (1999).*

Table 4. Thermal Properties of Polyurethane Foam

Temperature K	Thermal Cond cal/sec-cm-K	Specific Heat cal/g-K
100	1.4 E-04	0.303
296	1.4 E-04	0.303
323	1.5 E-04	0.324
373	1.6 E-04	0.358
423	1.8 E-04	0.440
473	2.0 E-04	0.475
523	2.2 E-04	0.526
3500	1.3 E-03	0.526

Table 5. Thermal Properties of Stainless Steel

Temperature K	Thermal Cond cal/sec-cm-K	Temperature K	Specific Heat cal/g-K
50	0.0300	50	0.096
200	0.0300	200	0.096
300	0.0325	300	0.114
400	0.0375	400	0.123
600	0.0450	600	0.133
750	0.0500	800	0.139
1100	0.0625	1000	0.146
2000	0.0900	1300	0.153
		3400	0.153

Given the physical parameters and boundary conditions, the computer model calculates the mass fraction (in the reactive foam block) and temperature as a function of location and time. A quantitative measure for comparison with experiment is the location of the decomposing front. The front is signified by the region where the solid fraction transitions from 1 (no decomposition) to 0 (fully decomposed). The location of the 0.5 solid fraction is plotted in Figure 7 for the model results corresponding to experiments with steady boundary temperatures, T_p, of 600 C, 750 C, and 900 C.

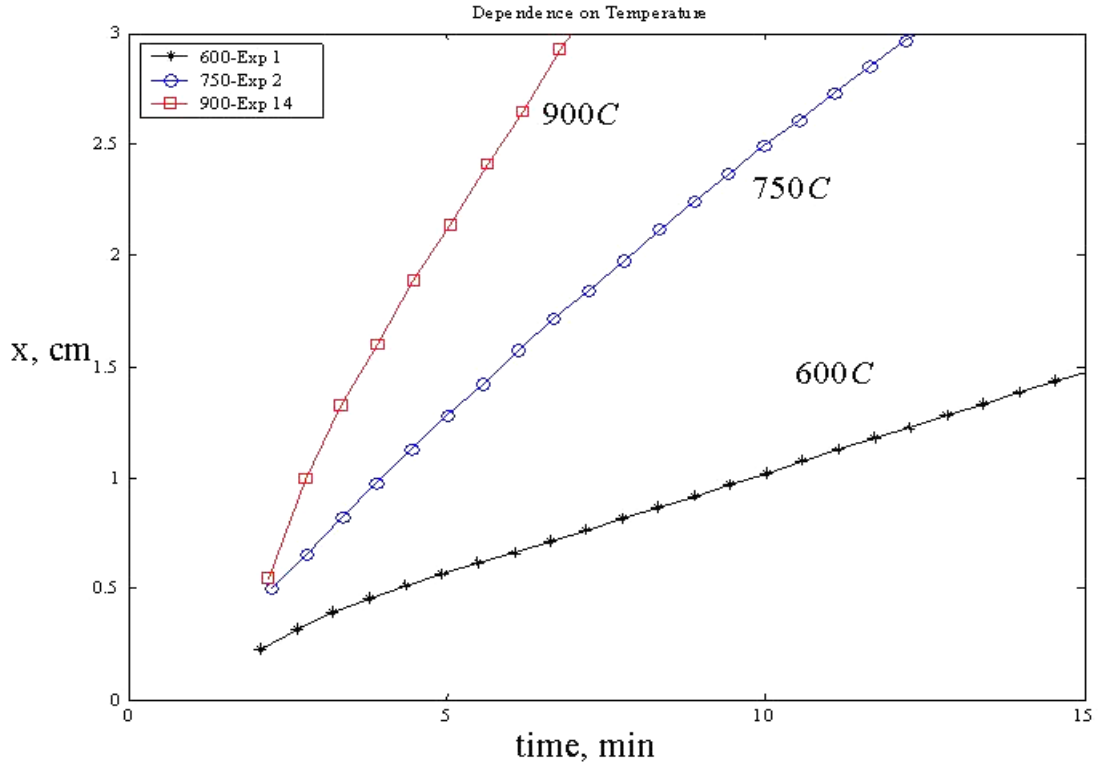

Figure 7. Model results for location of 0.5 solid fractions

Table 6 provides the model predictions for the validation data corresponding to the experimental results given in Table 1.

Table 6. Model results for Foam-in-can experiments

Experiment No.	Density (lb/ft^3)	Cup Plate Temperature	Orientation of Cup Plate	Component	Velocity (cm/min)
1	22.7	600 C	Bottom	None	0.0913
2	22.7	750 C	Bottom	None	0.2457
5	22.7	750 C	Bottom	Stainless Steel	0.2840
10	22.7	750 C	Top	None	0.2343
11	22.7	750 C	Side	None	0.2620
13	22.7	750 C	Side	None	0.2279
14	22.7	900 C	Bottom	None	0.4498
15	22.7	750 C	Bottom	Aluminum	0.2840
16	22.7	1000 C	Bottom	Stainless Steel	0.7698

This Page Intentionally Left Blank

VI. Model Calibration

General Approach

Model calibration involves the characterization of model parameters through estimation of an associated probability distribution. Values for parameters of the distributions were based on historical data (data from experimentation related to previous applications of the codes) and/or from calibration experimental data and expert opinion acquired for the present application. Twenty five parameters (those listed in Tables 2 and 3) were characterized in this fashion. Variability (or the impact of variability) in the remaining parameters (Tables 4, 5 and 6) was thought to be negligible by comparison. For this case study, we use results from the TGA experiments as calibration data for seventeen of the twenty five model parameters and rely on expert opinion for the remaining eight. There are a number of different methods for treatment of calibration data in the literature ranging from using only the estimated mean parameter value, to building all application-specific uncertainties into the characterization of the parameter distributions. A wide range for treatment of this aspect of the computational modeling process is illustrated in other analyses for this case study, see Easterling, (2002), and Hill et al., (2003). For a review of statistical methods used for calibration problems in general, see Campbell (2002).

The approach taken here is to utilize calibration information (including uncertainty estimates) concerning the expected value of the parameters, $\hat{\theta}$. We compute separately the unit-to-unit variability using the application-specific validation (benchmark) data. Consequently, when we perform the statistical analyses required in model validation, we are comparing experimental results to uncertain model predictions for the expected result, $E_\theta[m(\mathbf{x},\theta)]$. When we use the model for prediction, we start with an uncertain prediction and make uncertainty inferences based on the model uncertainty combined with other sources of variability estimated using the validation experiments. Our philosophy is to utilize all the calibration information we have about the model parameter predictions, but not to attempt the more difficult task of trying to infer how uncertainties and variabilities from other experiments "translate" to unit-to-unit variability for the present application. This approach is illustrated below for the polyurethane foam thermal decomposition case study.

Model Calibration for the Polyurethane Foam Decomposition Application – The Estimated Distribution *of* θ.

A first step in the process of calibrating model parameters involves fitting mathematical models using the calibration data. In our case, the models of interest are probability distributions for the expected values of these parameters. It is the expected value we wish to model using the calibration data because the test units in the TGA experiments are of entirely different size than those of interest in the application. As mentioned earlier, we try to estimate the unit-to-unit variation through the validation data instead.

For the present case study, some elements of θ are "fitted values" from 18 TGA experiments. The activation energies are parameters computed through an optimization process, fitting curves to the experimental results from the TGA experiments. The fitted values are used to estimate mean values for seventeen of the twenty-five model parameters used in the benchmark validation analysis. A further explanation of those experiments is given in Hobbs et al., (2002) and Dowding et al., (2003). The estimated variance-covariance matrix for the seventeen parameters Σ_θ is given in Dowding et al., (2003). We are interested in that matrix divided by 18 as the mean result $\hat{\theta}$ was estimated using 18 tests in the TGA experiments.

Next we extend Σ_θ to include variances for the remaining 8 parameters as provided by Hobbs et al., (2002). These parameters are assumed to be independent of each other and of the calibrated parameters. The estimated values for these parameters were provided to include variation among units. Our goal is only to capture variability in the expected (average) parameter values. There is no direct way to convert our information into an estimate for uncertainty related to the expected value of these parameters. To use the values provided would inflate the estimated modeling uncertainty. To continue with the analysis we have somewhat arbitrarily reduced these estimates by the same factor as the TGA data (variance/18). We emphasize the point that when expert judgment is being utilized, it is important to solicit estimates that are consistent with their intended use. This mean parameter estimate and the associated estimate of the covariance structure of the mean are listed in the appendix.

Model Calibration for the Polyurethane Foam Decomposition Application – Propagation of Model Uncertainty

A second step in the calibration process mathematical modeling for the response based on the estimated uncertainty distribution for $\hat{\theta}$. This propagation of uncertainty can be accomplished in a number of ways, including the following.

- For each **x** of interest, randomly sample, θ_i from the distribution $F(\theta)$ of the parameters and run the code $m(\mathbf{x},\theta_i)$. Repeat the process until the distribution of the response can be approximated with the desired accuracy.
- Estimate the change in response for a change in θ (from the mean value $\hat{\theta}$) for each **x** of interest. These derivatives can be used to replace the actual running of the code (above) by using $\frac{dy}{d\theta}\left(\theta' - \hat{\theta}\right) + m\left(\mathbf{x},\hat{\theta}\right)$ to get the approximate response for each element of the randomly generated set of parameter values θ.
- Use the derivatives mentioned above to obtain a first order approximation to the covariance structure of the responses. If it is reasonable to use a specific distribution for the response, then the covariance structure of the responses can be used in the estimation of distributional parameters.

More detail concerning these alternative approaches is provided in Hill, et al., (2003), and Dowding et al., (2003). These references provide a description of the process for estimating the "sensitivity" of the foam decomposition front location to the calibration parameters (as a function of time *t* and temperature *T*). In the appendix, we extend this approach to determine the covariance structure of velocity predictions made at different temperatures. Let $\frac{dl}{d\theta}(t,T)$ represent the derivative of front location as a function of the model parameters at time t and temperature T. These derivatives were approximated by running the code at points .01 $\hat{\theta}$ on either side of $\hat{\theta}$. They are available for temperatures 600°, 750°, and 900° only. We have described the first order approximations for computing the velocity covariance structure, in detail, in the appendix. Using these first order approximations, we obtain the mean vector, covariance matrix and correlation matrix for velocities:

$$[0.091 \quad 0.256 \quad 0.450], \begin{bmatrix} 0.00048 & 0.00006 & 0.00047 \\ 0.00006 & 0.00004 & 0.00012 \\ 0.00047 & 0.00012 & 0.00010 \end{bmatrix}, \text{ and } \begin{bmatrix} 1 & .40 & .68 \\ .40 & 1 & .61 \\ .68 & .61 & 1 \end{bmatrix}.$$

This mean vector and covariance structure apply to the expected response at the specified temperatures. The rows (and columns) of the matrices correspond to the three different temperatures. Note that there is substantial correlation between results at different temperatures, as we would expect. The other components of the input vector **x** (factors) are absence of the internal component and bottom heating orientation. These were the conditions for the units evaluated for derivatives. We show in the next section that these factors are not determined to be influential in the analysis. These parameters and transformations of them determined through the calibration process, are used in the next section for construction of test statistics and in the section on model-based prediction for predictions and the estimation of prediction uncertainty.

This Page Intentionally Left Blank

VII. Model Validation

General Approach

Model validation involves an assessment of the model based on comparison of the model predictions with the experimental data. The results of a model validation analysis are critical in providing direction for proceeding with the computational analysis. They are also important in providing feedback to model developers as indicated in Figure 1. We speak of validation of a model for a specific application. The question here is whether or not the codes can perform adequately for the application – a question that relies on the application requirements as well as comparison of responses to predictions for an answer. A number of outcomes are possible from this validation exercise. Boundaries between these outcomes, however, are not usually clear, and decisions on how to proceed are required on an application-by-application basis. Possible outcomes include:

- It is possible that data indicate the code is not capable of supporting the application.
- It is possible that data indicate the code can be used for the application but that supplementary modeling is needed to adjust model predictions in specific regions of the input space.
- It is possible that the data indicate no problem with using the model for the application.

When comparing model predictions to experimental results, the questions arise: What "pattern" of differences are we looking for? or In what way might we expect the two sets of responses to differ? There are some fairly obvious answers and some more difficult answers. We might look for:

a. a general lack of predictive capability for the model;
b. an overall bias in model predictions;
c. model biases that emerge with increasing or decreasing levels of specific inputs;
d. problems where the model scales one or more of the inputs incorrectly;
e. specific regions of the input space that are beyond the boundaries of the codes' applicability; and
f. other, application specific comparisons.

Testing for a lack of predictive power (a) can be addressed by comparing the variability in residuals (differences between experimental responses and model predictions) to variability in the experimental data alone. Similar variances indicate a lack of predictive capability in the code. The overall bias test (b) involves a test to see if mean differences between experimental and computational responses are significant. The input level and scaling biases (c) and (d) can often be identified through regression analysis or by looking for trends in the residuals. Looking for problematic regions in the input space (e) might be accomplished graphically or by using a "cluster" test statistic such as that discussed in Rutherford et al., (2003). Easterling, (2002) gives an example, for this case study, of an application-specific comparison (f).

The order indicated above is not necessarily the most efficient way for the statistical testing to proceed. In many cases it is desirable to look first for the more specific trends and/or effects, followed by (if appropriate and necessary) the more general hypothesis tests. It is important to note that there are a number of ways the model might fail to achieve its desired objectives. Testing to identify these problems should be performed in a systematic manner.

Model Validation for the Polyurethane Foam Decomposition Application – Statistical Testing

In this subsection, we outline the statistical testing performed in support of the foam decomposition analysis. Below is an outline of analyses and testing. Some discussion is provided in the paragraphs that follow with further detail deferred to the appendix. We:

- discuss appropriate variables for the statistical tests;
- discuss the predictive capability of the model;
- examine the possibility that heating orientation and presence/absence of a physical component affect velocities;
- test for a trend in the differences as a function of temperature T.

One other general issue regarding statistical testing relates to evaluating the test statistics. In the general hypothesis test setting, a test statistic is computed based on the data. The value of the statistic can be associated with a p-value that (in some sense) provides a standard way of reporting the results of the test. The p-value (see Bickel and Doksum (1977) for example) (typically) gives the probability (under the hypothesis being tested) of obtaining a test statistic value as high or higher in magnitude then the value achieved. Consequently, low p-values indicate an unlikely event casting doubt on the hypothesis. In the subsections below, we use p-values to indicate whether or not the statistical test provides significant evidence of discrepancies between experimental and computational results. One troubling aspect of hypothesis testing in these validation situations is that inadequate experimentation, either through poor experimental design or through too few tests performed, leads to less information and consequently to more difficulty in demonstrating evidence in the case where there really is a problem. It must be taken into account that limitations in experimentation lead to limits in our ability to identify problems even when they are quite substantial. A high p-value may be the result of insufficient information with which to make decisions reather than an indication of acceptable model performance.

Determining Appropriate Test Statistics

Following Easterling (2002) and Dowding et al. (2003), the statistical tests summarized here are performed using "log errors", computed as

d^* = ln(exp. result/prediction) or equivalently d^* = ln(exp. result) - ln(prediction)

where ln(.) is the natural logarithm. Logarithms were selected to help satisfy the assumptions of the statistical tests. Similar analyses indicate that it is quite common that the magnitude of the unit-to-unit differences is, on average, proportional to the mean response. Under this transformation and assumptions, the statistical testing and modeling effort is simplified substantially because the distribution of differences is assumed to be independent of temperature (an input that clearly affects the response (see Figure 8)).

Examining the Predictive Capability of the Model

The transformed responses and prediction are plotted as a function of temperature in Figure 8.

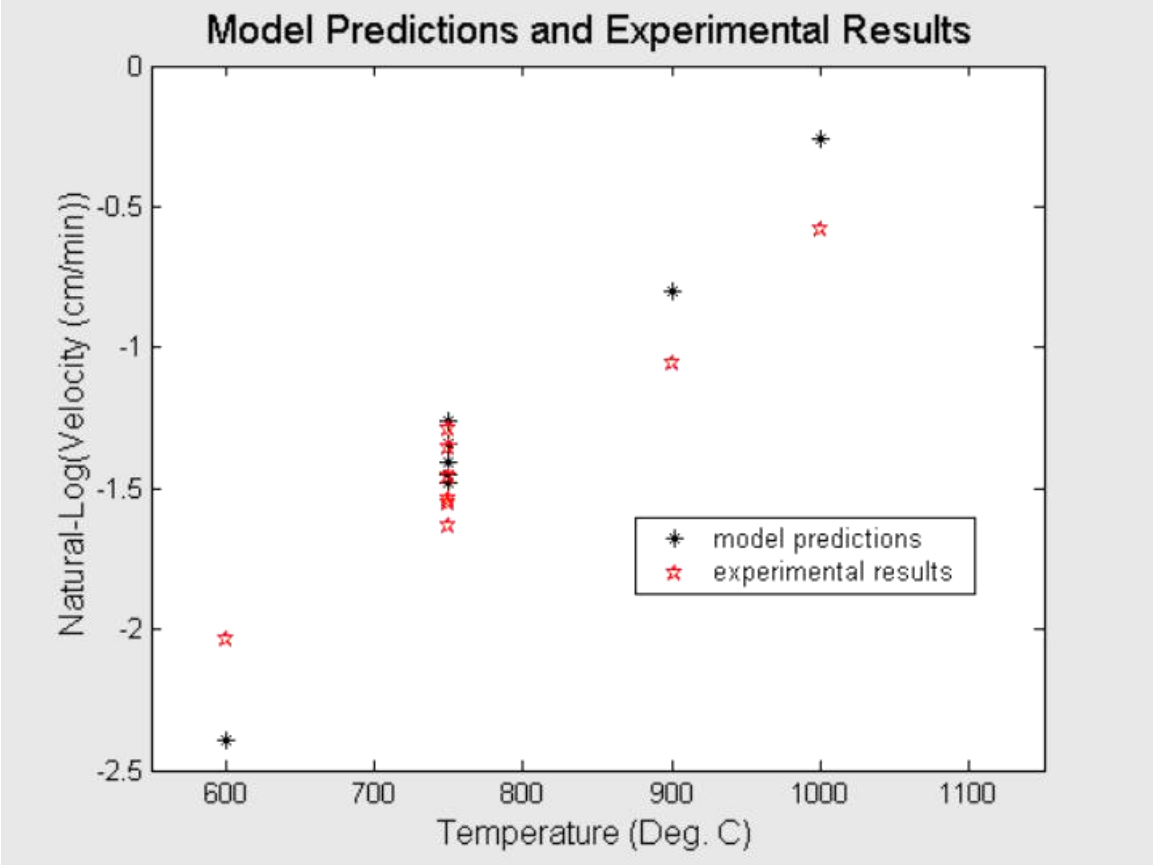

Figure 8. Plot of Natural Logarithms of the Velocity Data.

It is clear from Figure 8 that the model predictions display substantial predictive capability. The variability among differences is less than then the variability among experimental results alone. Whether or not these predictions are 'close enough" or whether another modeling approach might do better are decisions to be made based on the application requirements and alternative models. For this case study we have no guidance on this issue.

Examining the Possibility of Heating Orientation or Internal Component Effects

We mentioned earlier that the experimental design for the validation experiments included test units that differed because of the presence or absence of an internal component or the experimental setups differed because of a different heating orientation. These measured responses were compared with the base case response (750 C/Bottom/None) to see if these "factors" had an effect on the response. The temperature effect is examined in the next subsection. The question of an internal component effect is not examined here because it is not likely that the component would be influential at the locations 1 or 2 centimeters into the cylinder where data were extracted to calculate the velocities. The internal components may indeed affect other performance criteria.

Heating orientation was not altered for the model predictions. The only difference in the model calculations at 750 C (except for the internal component) was the boundary conditions associated with the thermal measurements conducted in the experiments and input into the model calculations. To examine the possibility of a heating orientation effect we perform an analysis of variance (ANOVA) using the log difference, d^*, results. The ANOVA table is included in the appendix. The p-value associated with these tests is .74 not indicating an effect associated with heating orientation.

Testing for a Linear Trend with Temperature

It is often the case that the statistical tests can be performed using theory associated with the general linear model. For the present case study, all tests are performed using this theory (see, for example, Graybill (1976)). Testing for a linear relationship between the log-differences and temperature was performed using a regression model that accommodates correlated data – the log-differences are correlated because model predictions are correlated at the three temperatures. We compute the appropriate covariance matrix using the model variability results of the previous subsection together with estimates of unit-to-unit variability based on the experimental results at 750 C.

The analysis of variance table is given in the appendix. The p-values associated with a linear coefficient is .12, indicating that there is a good chance of a significant linear trend in log-differences with temperature. We often use .05 or .1 as a "cut-off" for declaring significant differences in statistical tests. In the present situation, with so limited data, the p-value .12 is likely to indicate a quite substantial trend. It should be noted again that a lack of data or a poorly designed experiments generally reduces the chances of a low p-values making more difficult the recognition of model problems even when they are quite substantial. Every effort should be put forth to obtain meaningful data to validate the model.

Because of this likely deficiency in the model predictions and for illustration of the methodology for compensating for model biases we have included a model supplement term as discussed next. Our only justifiable statement about model validation through validation experiments is a "rough inference" because of the lack of data and design of the experiment. It appears that the model predictions tend to exaggerate the temperature effect for temperatures on either side of 750 C.

Construction of the Model Supplement Term

In this subsection, we describe the approach taken here for construction of the model supplement term $\eta(\mathbf{x})$ in expression (2). The apparent trend in differences between computational and experimental velocities as a function of temperature suggests that inclusion of this term will lead to better agreement with the experimental data and perhaps more accurate predictions. The challenges are to construct $\eta(\mathbf{x})$ so that, together with $m(\mathbf{x},\theta)$, they will yield unbiased predictions and to accurately assess the additional uncertainty introduced through inclusion of $\eta(\mathbf{x})$.

A model supplement term has been used in the validation literature in both Kennedy and O'Hagan, (2001) and Bayarri et al., (2002). The methodology used in these papers for a Bayesian approach to building random function models, however, dates back to Carren et al., (1993), and other references provided in Kennedy and O'Hagan (2001).

The approach taken here is referred to as the "response-modeling approach," see Rutherford (1999). It is used for this case study because of the flexibility it provides in assessing performance characteristics associated with the velocities. The reliability prediction discussed in the next section gives a demonstration of the general applicability of the approach. A brief summary of response modeling is included in the appendix.

Figure 9 illustrates the response model for this application. The "realizations" or curves indicate "likely" values of the differences (not log differences – they were used only for the statistical tests) between experimental velocities and model predictions. Differences between realizations indicate the uncertainty associated with this component of the predictive models (see expression (2)). Some of the difficulties associated with this approach to building a model supplement component are also addressed as the final topic in the appendix.

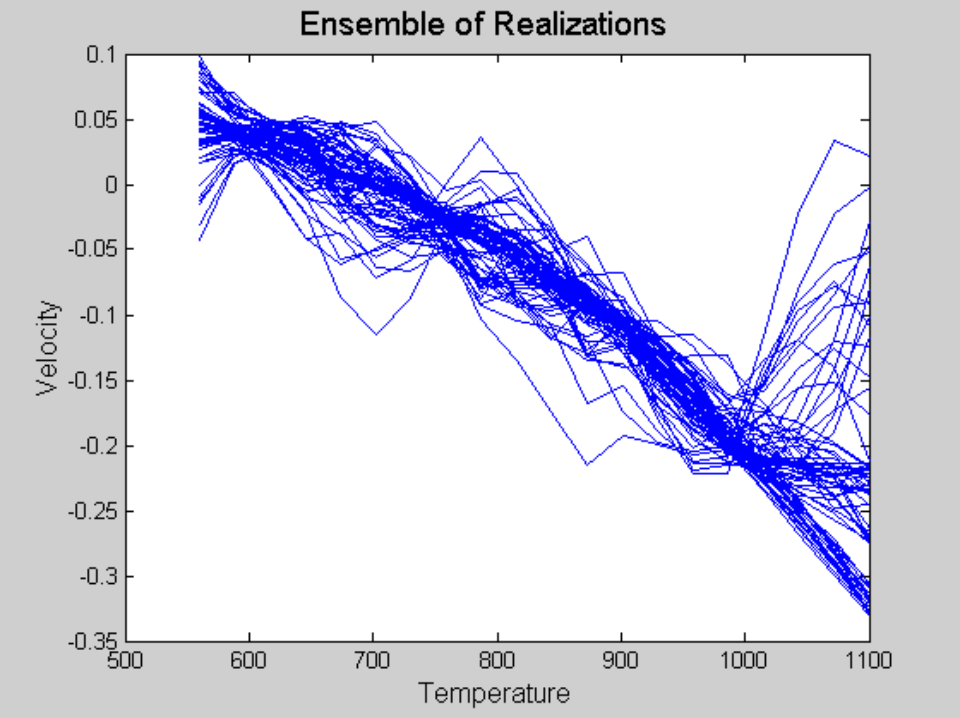

Figure 9. Realizations for the Response Model of Differences Between Experimental Results and Model Predictions.

VIII. Model-Based Prediction

General Approach

Model-based prediction involves utilizing the code and possibly supplemental modeling to make predictions. The predictions may be point predictions – individual responses at points (in the input space) where validation data are not available or more general predictions involving functions of multiple input points or some region of the input space. The model supplement term is used to adjust predictions in regions of the input space where the model validation results indicate prediction biases. As the code development effort evolves, the need for this additional modeling should diminish.

For the present case study, no specific prediction requirements were specified. For illustration, we consider hypothetical prediction requirements:

1) Interpolation – prediction of the response at temperature T=850 C
2) (Minor) Extrapolation – prediction of the response at T=1100 C
3) Averaging – prediction of the average response assuming equally likely temperature values in the application.
4) Reliability – we (arbitrarily) select a threshold velocity, assume that velocities exceeding this threshold created a possible "failure" situation and estimate reliability, assuming again equally likely temperature values.

These problems are addressed in the last four subsections of this section. Details concerning the predictive models are given below.

The predictions and part of the related uncertainty are based on the modeling terms described in the previous section. For prediction at point $\mathbf{x}''$,

$$E_\theta[m(\mathbf{x}'',\theta)] = \int m(\mathbf{x}'',\theta) f(\theta) d\theta .$$

When it is determined the model is not performing adequately, the model supplement term $\eta(\mathbf{x}'')$ is required. The predictions are adjusted by the quantity $\eta(\mathbf{x})$

$$E_\theta[m(\mathbf{x}'',\theta)] + \eta(\mathbf{x}'').$$

Uncertainty for the "adequate-model" prediction would be calculated using the variance

$$Var_\theta[m(\mathbf{x}'',\theta)] = \int (m(\mathbf{x}'',\theta) - E_\theta[m(\mathbf{x}'',\theta)])^2 f(\theta) d\theta .$$

When a model supplement term is included, its uncertainty is accounted for through the variance estimate

$$Var_\theta[m(\mathbf{x}'',\theta)] + Var\,(\eta(\mathbf{x}''))$$

where variance in $\eta(\mathbf{x}'')$ is captured through the response modeling process described earlier and in the appendix.

When $m(\mathbf{x},\theta)$ and $\eta(\mathbf{x})$ are combined, the resulting distribution characterizes uncertainty in the predicted mean of the response. Variability in the unit-to-unit response is captured through the term $e_i(\mathbf{x})$.

Combining the Uncertainties

The three sources of uncertainty for the components of expression (2) (repeated below) are given in Figure 10.

$$p(\mathbf{x}) = m(\mathbf{x},\theta) + \eta(\mathbf{x}) + e(\mathbf{x}) \qquad (2)$$

The first figure in Figure 10 relates to uncertainty in $m(\mathbf{x},\theta)$ at temperatures 600 C, 750 C and 900 C. The bounds shown 80% (green) and 90% (blue) are constructed assuming a normal distribution for model uncertainty. The second figure is computed from the ensemble of supplemental responses representing the term $\eta(\mathbf{x})$ as described in the previous section. The green and blue bounds are again 80% and 90% bounds constructed, in this case, by indicating the region containing that portion of the realizations. The third plot addresses unit-to-unit response variability estimated using the experimental data at 750 C and assuming constant variance, normally distributed ln(e_i) and consequently a lognormal distribution of unit-to-unit responses. Note that the uncertainty (or variability) characterized for the three terms is quite similar in magnitude (the velocity scale covers a range of .9 cm/min in each plot).

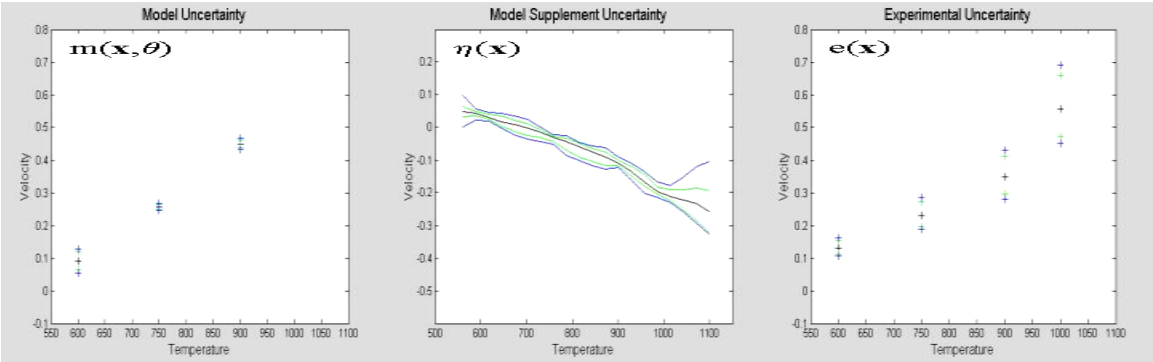

Figure 10. Sources of Uncertainty in Model Predictions.

Uncertainty for the three sources is combined and illustrated in Figure 11. Realizations displaying uncertainties indicated in the first and third plot in Figure 10 (but centered at zero) are generated under the assumptions given above. These realizations are then combined with those in the second figure and added to the model-predicted response.

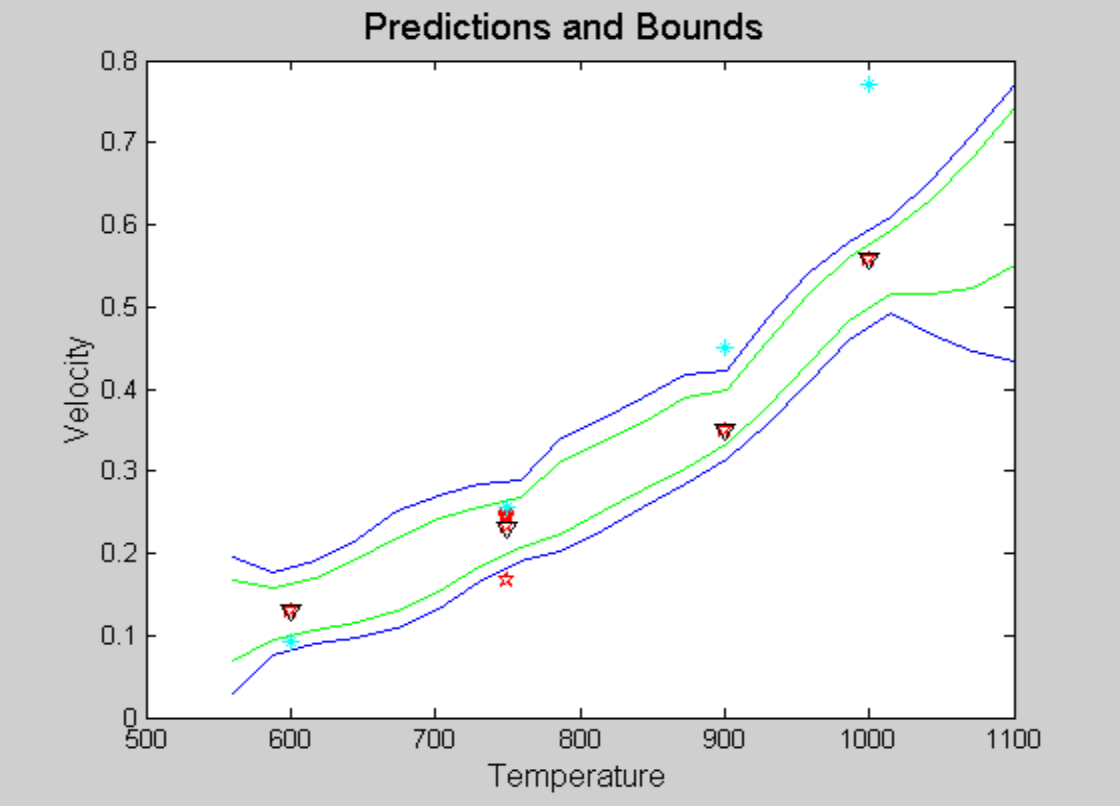

Figure 11. Velocity Predictions, 80% (green), and 90% (blue) Bounds. The model predictions are the light blue stars; the data are the red stars and the data averages at each temperature are indicated by the black triangles.

The bounds in Figure 11 are to be interpreted pointwise as bounds on point predictions. There is substantial correlation among predictions and consequently, coverage probabilities over the entire range of temperatures may be fairly accurate on average (over repeated analyses) but are quite variable and are likely to appear inaccurate in coverage probability over any interval range of temperature. We now proceed to the specific predictions described earlier.

Bounds at 850 C

Bounds for our first two prediction problems can be determined directly from the plot in Figure 11. At 850 C, the histogram plotted in Figure 12 indicates realization values at T=850 C. In general, the histogram could be replaced with a probability density estimate and the desired probabilities could be estimated. The 90% prediction bounds indicated in Figure 12 are obtained by taking the appropriate percentiles. The interpretation of the interval [.28 , .45] is that approximately 90% (on average) of the units tested at 850 C will have velocities falling within this interval.

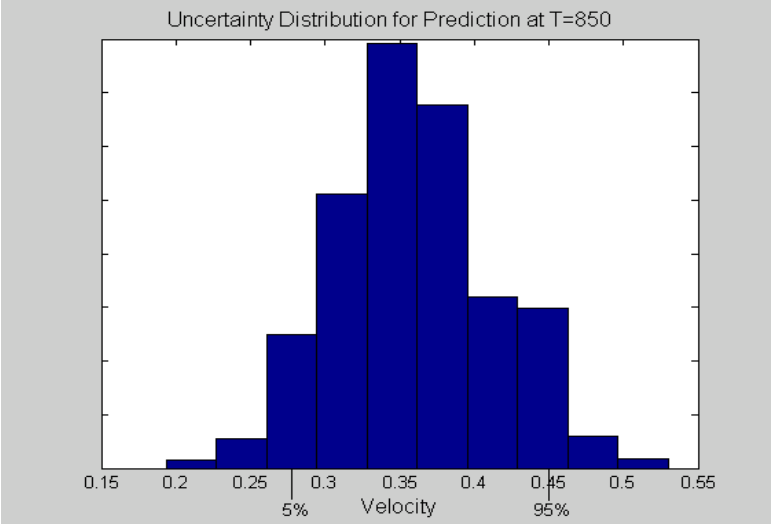

Figure 12. Histogram Indicating Predictions and Prediction Uncertainty at *T*=850 C.

Bounds at 1050 C

At 1050 C, the histogram is plotted in Figure 13. The 90% prediction bounds are computed as they were for the previous problem and the interpretation is similar. Note that the bounds at *T*=1050 C are substantially wider than those at 850 C. The primary reason for this is that there is less information at higher temperatures to "pin down" the estimate and related uncertainty.

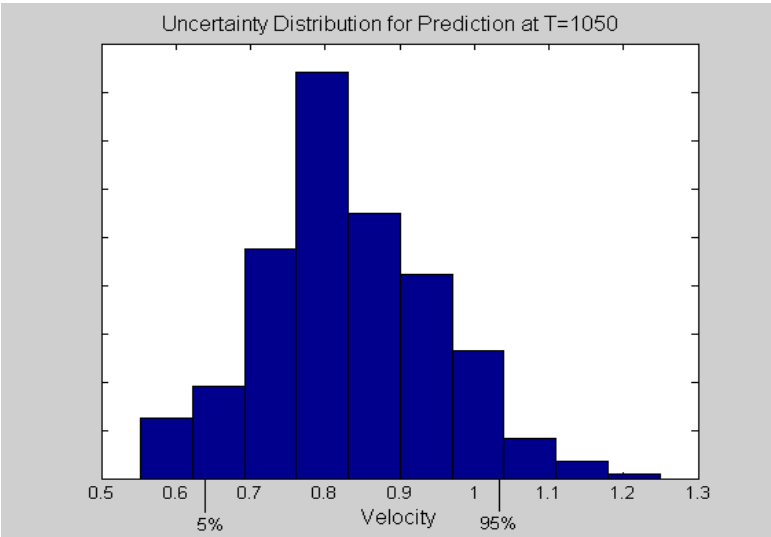

Figure 13. Histogram Indicating Predictions and Prediction Uncertainty at *T*=1050 C.

Bounds on the Average Velocity

The histogram of results for average velocity is shown in Figure 14. Averages are computed for each realization in the ensemble. The computation is made assuming probabilities for the actual fire temperatures are uniformly distributed between 600 C and 1050 C. Other assumptions regarding the distribution of temperatures in 'likely' fire scenarios could be easily accommodated.

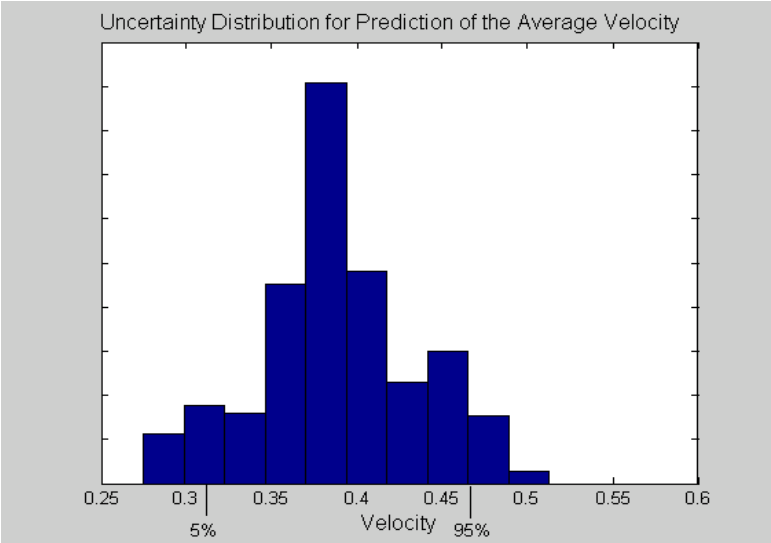

Figure 14. Histogram Indicating Predictions and Prediction Uncertainty for Average Velocity.

Bounds on Reliability

For this final prediction problem, we assume that velocities above .95 cm/min would lead to "failure". Failure probabilities are then computed over each realization. The histogram of reliability results is plotted in Figure 15.

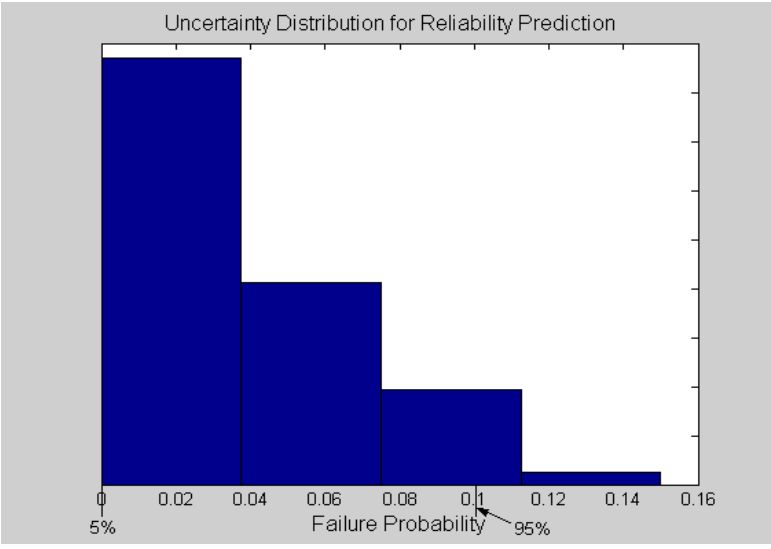

Figure 15. Histogram Indicating Predictions and Prediction Uncertainty for the Hypothetical Reliability Prediction.

This Page Intentionally Left Blank

IX. Summary

In this report we have provided a fairly detailed account of one approach to model validation and its application to a polyurethane thermal foam decomposition case study. We discussed several elements of the "philosophy" behind the approach.

In the analysis it is determined that the model predictions may tend to "exaggerate" the effect of temperature changes when compared to the experimental results. To compensate for this, a model supplement term was constructed and used in the remainder of the analysis. Several hypothetical prediction problems were addressed. Hypothetical problems are used because no guidance was provided on this aspect of the case study. The resulting predictions and corresponding uncertainty assessment demonstrate the flexibility of the approach.

A number of decisions regarding objectives and assumptions were made for this presentation. In some cases these decisions were made in order to illustrate methodology for the purpose of demonstration for future validation applications. There were no definitive results given here regarding the use of the COYOTE model for this application.

This Page Intentionally Left Blank

References

Bayarri, M. J., Berger, J. O., Higdon, D., Kennedy, M. C., Kottas, A., Paulo, R., Sacks, J., Cafeo, J. A., Cavendish, J., Lin, C. H. and Tu, J. (2002), 'A Framework for Validation of Computer Models', V&V Foundations, October 2002.

Bickel, P. J. and Doksum, K. A. (1977), 'Mathematical Statistics: Basic Ideas and Selected Topics', Holden Day Inc., San Francisco.

Bury K. V. (1977) 'Statistical Models in Applied Science',Krieger Publishing Co., Huntington, New York.

Deutsch, C. V. and Journel, A. G. (1998), 'GSLIB Geostatistical Software Library and Users Guide Second Edition', Oxford University Press, New York.

Dobranich, D. and Gill, W., (1999), 'Thermal Simulations and Experiments for the W76 AF&F Assembly – An Integrated Approach', SAND99-1925, Sandia National Laboratories, Albuquerque, New Mexico.

Campbell, K. (2002), 'A Brief Survey of Statistical Model Calibration Ideas', LA-UR-02-3157, Los Alamos National Laboratory, New Mexico.

Dowding, K. J., Hills, R. G., Leslie, I., Pilch, M. and Rutherford, B. M., (2003) 'An Initial Validation Methodology for Abnormal Environments: Assessing a Model for Thermal Decomposition of Polyurethane Foam', , SAND2003-XXXX (in progress), Sandia National Laboratories, Albuquerque, New Mexico.

Easterling, R. G. (2002), 'Measuring Predictive Capability of Computational Models: Foam Case Study', SAND2003-0287, Sandia National Laboratories, Albuquerque, New Mexico.

Graybill, F. A. (1976), 'Theory and Application of the Linear Model', Duxbury Press, North Scituate, Massachusetts.

Hills, R. G., Leslie, I. H. and Dowding, K. (2003), 'Statistical Validation of Engineering and Scientific Models: Application to the Abnormal Environment', SAND2003-XXXX (in progress); Sandia National Laboratories, Albuquerque, New Mexico.

Hobbs M. L., Erickson, K. L., Chu, T. Y., Borek, T. T., Thompson, K. R., Dowding, K. J., Clayton, D. and Fletcher, T. H. (2003) "CPUF – Chemical Structure-based Polyurethane Decomposition Model," SAND2003- XXXX (in progress), Sandia National Laboratories, Albuquerque, New Mexico.

Iman, R. L. and Conover, W. J. (1982), 'A Distribution-Free Approach to Introducing Rank Correlation Among Input Variables', *Communications in Statistics, Part B - Simulation & Computation*, 11(3), pp. 311-334.

Kennedy, M. C., and O'Hagan, A. (2002), 'Bayesian Calibration of Computer Models' (with discussion), *Journal Of The Royal Statistical Society (Series B),* 58, pp.425-464.

McKay, M. D., Beckman, R. J. and Conover, W. J. (1979), 'A Comparison of Three Methods for Selecting Values of Input Variables in the Analysis of Output from a Computer Code', *Technometrics*, Vol. 21, No. 2, pp. 239-245.

O'Connell, M. A., and Wolfinger, R. D. (1997), 'Spatial Regression Models, Response Surfaces, and Process Optimization', *Journal of Computational and Graphical Statistics*, Vol. 6, No. 2, pp. 224-241.

Rutherford, B. (2000), 'An Algorithmic Approach to Experimental Design for the Computer Analysis of a Complex System', SAND2000-0871, Sandia National Laboratories, Albuquerque, New Mexico.

Rutherford, B. (2002), 'A Response-Modeling Approach to Computer Experimental Design', Whitepaper , Sandia National Laboratories, Albuquerque, New Mexico.

Sacks, J., Welch, W. J., Mitchell, T. J. and Wynn, H. P. (1989), 'Design and Analysis of Computer Experiments' *Statistical Science*, Vol. 4, No. 4, pp. 409-423.

Trucano, T. G., Pilch, M. and Oberkampf W. L. (2002), 'General Concepts for Experimental Validation of ASCI Code Applications', SAND2002-0341, Sandia National Laboratories, Albuquerque, New Mexico.

Trucano, T. G., Easterling, R. G., Dowding, K. Paez, T. L.,Urbina, A., Romero, V. J. and Rutherford, B. M. (2001), 'Description of the Sandia Validation Metrics Project', SAND2001-1339, Sandia National Laboratories, Albuquerque, New Mexico.

U.S. Department of Energy Defense Programs (2000) 'Accelerated Strategic Computing Initiative (ASCI) Program Plan,' DOE/DP-99-000010592.

Appendix

Overview

This appendix provides technical details for several of the statistical tests and procedures used in this case study analysis. Sections of the appendix are ordered as they are referenced in the text. Separate sections are included for:

Calibration – Propagation of uncertainty in model parameters to velocity predictions;
Model Validation – Analysis of variance results for significance tests for inputs in the benchmark data analysis; and
Model-based Prediction – Overview of response modeling and performance issues.

Estimating the Variance-Covariance Structure for Velocities Using the TGA Data

The model parameter values established primarily through the TGA experimental data are given by:

$\theta =$ [50209 50567 49374 50408 49985 49508 50397 49276 51513 49791 50195 50147 50201 51081

49608 49730 3521.4 300 0.78 0.364 1 20.6 0.8 2.8 0.036]

The variance-covariance matrix Σ_θ, is listed below. The matrix is given in two sections corresponding to parameters 1-17 and 18-25. The diagonal values in the second section of the matrix, rows and columns 18-25, were provided through expert judgment as described in Section VI. These variance values were (somewhat arbitrarily) divided by 18, as were the TGA results (the TGA results were based on 18 experiments). Alteration of the expert-provided values was considered necessary because the estimates were provided to include unit-to-unit variability (see Hobbs et al., (2003)). Sections of the matrix not shown are zeros..

Their variance-covariance matrix is given by: $\Sigma_\theta =$

3.2E+03	1.9E+03	-1.1E+03	1.6E+03	7.2E+02	-8.3E+00	6.7E+02	-9.6E+02	-6.3E+02	1.5E+03	-1.6E+03	1.3E+03	-1.5E+03	2.4E+03	2.1E+03	8.0E+01	-5.1E+01
1.9E+03	2.2E+03	-1.0E+03	1.6E+03	1.1E+03	-8.3E+02	7.1E+02	-1.1E+03	-1.2E+03	1.2E+03	-9.3E+02	2.0E+03	-1.3E+03	1.7E+03	1.2E+03	3.0E+02	-6.2E+01
-1.1E+03	-1.0E+03	6.4E+02	-8.2E+02	-5.4E+02	-1.9E+02	-2.2E+02	3.8E+02	6.1E+02	-7.4E+02	7.4E+02	-7.4E+02	7.7E+02	-1.1E+03	-7.6E+02	3.8E+01	2.3E+01
1.6E+03	1.6E+03	-8.2E+02	1.3E+03	7.5E+02	-3.9E+02	5.1E+02	-7.8E+02	-9.0E+02	9.1E+02	-7.9E+02	1.5E+03	-1.0E+03	1.3E+03	8.8E+02	2.2E+02	-5.6E+01
7.2E+02	1.1E+03	-5.4E+02	7.5E+02	9.5E+02	-1.5E+00	2.3E+02	-4.0E+02	-7.2E+02	7.2E+02	-5.8E+02	7.3E+02	-7.9E+02	8.8E+02	5.8E+02	-5.9E+01	-1.6E+01
-8.3E+00	-8.3E+02	-1.9E+02	-3.9E+02	-1.5E+00	2.5E+03	-6.2E+02	8.8E+02	1.6E+02	2.5E+02	-7.6E+02	-1.8E+03	-7.7E+01	1.6E+02	3.4E+02	-8.0E+02	4.0E+01
6.7E+02	7.1E+02	-2.2E+02	5.1E+02	2.3E+02	-6.2E+02	3.4E+02	-4.7E+02	-2.6E+02	2.5E+02	-1.5E+02	7.4E+02	-3.1E+02	4.2E+02	2.9E+02	2.6E+02	-3.2E+01
-9.6E+02	-1.1E+03	3.8E+02	-7.8E+02	-4.0E+02	8.8E+02	-4.7E+02	6.8E+02	4.6E+02	-4.4E+02	2.6E+02	-1.2E+03	5.3E+02	-7.0E+02	-4.7E+02	-3.3E+02	4.2E+01
-6.3E+02	-1.2E+03	6.1E+02	-9.0E+02	-7.2E+02	1.6E+02	-2.6E+02	4.6E+02	9.0E+02	-6.5E+02	4.7E+02	-1.2E+03	7.4E+02	-7.1E+02	-3.6E+02	-9.8E+01	3.8E+01
1.5E+03	1.2E+03	-7.4E+02	9.1E+02	7.2E+02	2.5E+02	2.5E+02	-4.4E+02	-6.5E+02	9.8E+02	-9.6E+02	8.2E+02	-1.0E+03	1.4E+03	1.1E+03	-1.2E+02	-1.7E+01
-1.6E+03	-9.3E+02	7.4E+02	-7.9E+02	-5.8E+02	-7.6E+02	-1.5E+02	2.6E+02	4.7E+02	-9.6E+02	1.1E+03	-2.8E+02	9.4E+02	-1.4E+03	-1.2E+03	2.5E+02	1.1E+01
1.3E+03	2.0E+03	-7.4E+02	1.5E+03	7.3E+02	-1.8E+03	7.4E+02	-1.2E+03	-1.2E+03	8.2E+02	-2.8E+02	4.0E+03	-1.0E+03	9.6E+02	5.8E+02	6.1E+02	-1.1E+02
-1.5E+03	-1.3E+03	7.7E+02	-1.0E+03	-7.9E+02	-7.7E+01	-3.1E+02	5.3E+02	7.4E+02	-1.0E+03	9.4E+02	-1.0E+03	1.0E+03	-1.4E+03	-1.1E+03	5.2E+01	2.4E+01
2.4E+03	1.7E+03	-1.1E+03	1.3E+03	8.8E+02	1.6E+02	4.2E+02	-7.0E+02	-7.1E+02	1.4E+03	-1.4E+03	9.6E+02	-1.4E+03	2.4E+03	1.9E+03	-1.6E+02	-5.9E+00
2.1E+03	1.2E+03	-7.6E+02	8.8E+02	5.8E+02	3.4E+02	2.9E+02	-4.7E+02	-3.6E+02	1.1E+03	-1.2E+03	5.8E+02	-1.1E+03	1.9E+03	1.6E+03	-1.9E+02	1.9E+00
8.0E+01	3.0E+02	3.8E+01	2.2E+02	-5.9E+01	-8.0E+02	2.6E+02	-3.3E+02	-9.8E+01	-1.2E+02	2.5E+02	6.1E+02	5.2E+01	-1.6E+02	-1.9E+02	3.5E+02	-3.4E+01
-5.1E+01	-6.2E+01	2.3E+01	-5.6E+01	-1.6E+01	4.0E+01	-3.2E+01	4.2E+01	3.8E+01	-1.7E+01	1.1E+01	-1.1E+02	2.4E+01	-5.9E+00	1.9E+00	-3.4E+01	1.5E+01

for the first seventeen parameters and the uncorrelated diagonal matrix below for the remaining eight parameters.

5.00E-01	0.00E+00	0.00E+00	0.00E+00	0.00E+00	0.00E+00	0.00E+00	0.00E+00
0.00E+00	1.39E-04	0.00E+00	0.00E+00	0.00E+00	0.00E+00	0.00E+00	0.00E+00
0.00E+00	0.00E+00	7.22E-05	0.00E+00	0.00E+00	0.00E+00	0.00E+00	0.00E+00
0.00E+00	0.00E+00	0.00E+00	5.56E-04	0.00E+00	0.00E+00	0.00E+00	0.00E+00
0.00E+00	0.00E+00	0.00E+00	0.00E+00	2.33E-01	0.00E+00	0.00E+00	0.00E+00
0.00E+00	0.00E+00	0.00E+00	0.00E+00	0.00E+00	1.39E-04	0.00E+00	0.00E+00
0.00E+00	0.00E+00	0.00E+00	0.00E+00	0.00E+00	0.00E+00	4.33E-03	0.00E+00
0.00E+00	0.00E+00	0.00E+00	0.00E+00	0.00E+00	0.00E+00	0.00E+00	2.67E-06

Using a first order approximation, (see Bury (1986), for example) we can obtain the variance-covariance matrix for decomposition front location corresponding to the front movement from 1 cm to 2 cm as

$$\sum_f = \begin{bmatrix} \frac{dl}{d\theta}(10,600) \\ \frac{dl}{d\theta}(21,600) \\ \frac{dl}{d\theta}(3.9,750) \\ \frac{dl}{d\theta}(7.8,750) \\ \frac{dl}{d\theta}(2.8,900) \\ \frac{dl}{d\theta}(4.8,900) \end{bmatrix} \sum_\theta \begin{bmatrix} \frac{dl}{d\theta}(10,600) \\ \frac{dl}{d\theta}(21,600) \\ \frac{dl}{d\theta}(3.9,750) \\ \frac{dl}{d\theta}(7.8,750) \\ \frac{dl}{d\theta}(2.8,900) \\ \frac{dl}{d\theta}(4.8,900) \end{bmatrix}'$$

The first arguments in the parentheses above represent the times the fronts passed 1 cm and 2 cm for predicted results at the specified temperature. The temperatures are the second argument in the parentheses. The first, third and fifth component of each vector is for 1 cm.; the remainder are for 2 cm.

Next, to estimate the variance-covariance relationship for velocities:

$$\sum_v = \begin{bmatrix} \frac{-1}{11} & \frac{1}{11} & 0 & 0 & 0 & 0 \\ 0 & 0 & \frac{-1}{3.9} & \frac{1}{3.9} & 0 & 0 \\ 0 & 0 & 0 & 0 & \frac{-1}{2} & \frac{1}{2} \end{bmatrix} \sum_f \begin{bmatrix} \frac{-1}{11} & \frac{1}{11} & 0 & 0 & 0 & 0 \\ 0 & 0 & \frac{-1}{3.9} & \frac{1}{3.9} & 0 & 0 \\ 0 & 0 & 0 & 0 & \frac{-1}{2} & \frac{1}{2} \end{bmatrix}' .$$

The matrices specified above transform the front location covariance structure for front location to velocities. The components of the matrices are the reciprocal of the times the decomposition fronts take to travel from 1 cm. to 2 cm. The resulting mean and variance-covariance matrix for velocities are:

$E_\theta[m(\mathbf{x},\theta)] =$ [0.091 0.256 0.450] and

$$\sum_{v} = \begin{bmatrix} 0.00048 & 0.00006 & 0.00047 \\ 0.00006 & 0.00004 & 0.00012 \\ 0.00047 & 0.00012 & 0.00010 \end{bmatrix}$$

and the associated correlation matrix is:

$$\begin{bmatrix} 1 & 0.40 & 0.68 \\ 0.40 & 1 & 0.61 \\ 0.68 & 0.61 & 1 \end{bmatrix} .$$

Finally, our statistical tests compare log(predictions) to log(exp. results). We need to identify the associated distribution for d^* that will yield the above mean values and variance-covariance structure. For $\ln(m(\mathbf{x},\theta_i))$ we get:

$$E_\theta(\ln(m(\mathbf{x},\theta))) = [-2.43 \ \ -1.36 \ \ -.80]$$

and covariance

$$\sum_{\ln(v)} = \begin{bmatrix} .0565 & .00255 & .0128 \\ .00255 & .0006 & .00116 \\ .0128 & .00116 & .0052 \end{bmatrix}.$$

Values for the covariance matrix were approximated using a rough optimization procedure. This mean and covariance were used in the statistical test for temperature effects discussed below.

Analysis of Variance Tables for the ANOVA Analyses and Regression

Statistical tests were performed to infer whether or not there was enough evidence in the limited data to declare significant differences as a result of the factors (orientation and temperature) in the analysis. The analysis of variance (ANOVA) tables for these two analyses are presented here for completeness. A discussion of the interpretation and theory behind these tables is given in any statistical text covering analysis of variance and regression. The ANOVA table giving results for testing for significant heating orientation effects follows:

Source	df	SS	MS	F	*p*-value
Orientation	2	0.0163	0.0081	0.33	0.740
Error	3	0.0731	0.0244		

.

In examining the differences *d** for a linear trend in velocity with temperature, we have a set of correlated results (because of the correlated model predictions) that we assume, for the statistical tests, are normally distributed with parameters described in the previous subsection. The covariance matrix is obtained by adding the experimental variance to the diagonal elements of the model covariance structure $\sum_{\ln(v)}$.

The basic linear model tested here is $d_i^* = \beta_o + \beta_1 T$. We test the hypothesis $\beta_1 = 0$ (i.e. there is no significant trend in the log differences due to change in temperature).

The ANOVA table giving results for testing for significant temperature effect follows:

Source	df	SS	MS	F	*p*-value
Temperature	1	2.99	2.99	3.37	.12
Error	6	5.34	0.89		

Overview of the Response Modeling Approach to Response Characterization

Response models are used in this case study to characterize differences between prediction and experimental results. Response models have been used for more than a decade in geo-science areas to characterize physical regions in two- and three-dimensions, see Deutch and Journal (1998), Chapter V and their references. The terminology "stochastic simulation" is used there to describe a variety of approaches to constructing "typical", or what they called "equal probable" realizations that were then used to obtain performance characteristics related to the site. We use this discrete ensemble in a similar way, but construction is more in the spirit of a Latin Hypercube sample, McKay, Beckman, and Conover (1979), where the realizations are generated to span the response range while attempting to satisfy the consistency property stated below.

The method used here for constructing the response-model consists of generating an ensemble of hypothetical response surfaces (the realizations) conditioned on the data. The response ensemble **r** consists of a set of *k* realizations $\mathbf{r} = \left(r^i(\mathbf{x}), i = 1,...,k\right)$ where **x** is any point in the input space. Ideally, **r** is constructed in a manner consistent with the data $\mathbf{y} = y(\mathbf{x}_i)$, i=1,…,n in the following sense: for any given region, *R* of the response space, if the conditional probability $P(r \varepsilon R \mid \mathbf{y}) = p$ then the expectation of the number of realizations $r^i(\mathbf{x})$ in *R*, taken over repeated application of the response-modeling process, is *kp*.

The assertion $P(r \varepsilon R \mid \mathbf{y}) = p$ is somewhat vague and requires assumptions for a mathematical formalization. Decisions regarding the modeling assumptions are necessarily somewhat arbitrary. Rutherford (1999, 2002) address some of the issues, others are the topic of our current research. Clearly, there are a number of elements of approximation in the construction of the ensemble itself and of the individual realizations. In our experience, however, this has been a useful tool in spite of these assumptions and approximations.

Rutherford (1999, 2002) discuss the mathematical form and method of construction for the individual realizations. Briefly, a model is assumed of the form:

$$r(T) = \beta_o + \beta_1 T + \beta_2 T^2 + \xi(T) = P(T) + \xi(T) \qquad \text{(A1)}$$

The term $P(T)$ represents a polynomial in T (temperature) and $\xi(T)$ represents a Gaussian random function (see Sacks, Welch, Mitchell and Wynn (1989) and their references), defined using a stationary spatial covariance function:

$$C(T,T') = C(|T - T'|) = e^{-\phi|T-T'|^{\tau}} \qquad \text{for any } T \text{ and } T'.$$

Some of the considerations related to these modeling choices are discussed in O'Connell and Wolfinger (1997).

We tried three different polynomial models (alternatives for $P(T)$ in equation A1) – constant, linear, and quadratic. No guidance is provided on which model is appropriate and the model selection does make a difference. Figure A1 shows the realizations modeling $\eta(T)$ uncertainty. One clear trade-off is between the range of uncertainty and the degree of the polynomial. If one is willing to assume that the relationship is close to quadratic (an assumption very likely to appear reasonable when so few data are available), then the random function portion of the response model ξ is based on small residuals and, consequently, the realizations are relatively tight. Conversely, when the polynomial model consists of only an overall constant, the residuals are large and the realizations are relatively dissimilar. Note further, that when only a constant is assumed, the realizations tend toward the mean with no "structural support" as temperatures fall outside the range of the data. This can clearly have undesirable consequences for predictions involving extrapolation. A cross-validation analysis was performed measuring the likelihood of one data point (difference) at a time while the modeling was based on all data except that point. The analysis tended to favor the constant model slightly. Questions about extrapolation, however, make it less attractive. For this case study, we combined the three sets of realizations. In the future, one would hope to have more data to help discriminate between response models. Constructing $\eta(\mathbf{x})$ for the present case study illustrates some of the problems likely to repeat themselves in model validation applications in the future – there are too few data to make reasonable estimates of the required modeling parameters. Figure A1 illustrates the problem.

Constructing the realizations is accomplished by first establishing the polynomial component. The βs and their variance-covariance structure are estimated using the raw differences. The polynomial portion of each realization is determined by sampling from the distributions of βs (assuming a normal distribution) using Latin hypercube sampling adjusted to induce a rank correlation matching the estimated correlation in the βs (see Iman and Conover (1982)). Through this approach, we force the polynomials to span the response range. The random function component $\xi(T)$, for each realization, is generated using the sequential-Gaussian simulation approach, (Deutsch and Journel (1998)) using the residuals of the polynomial fit.

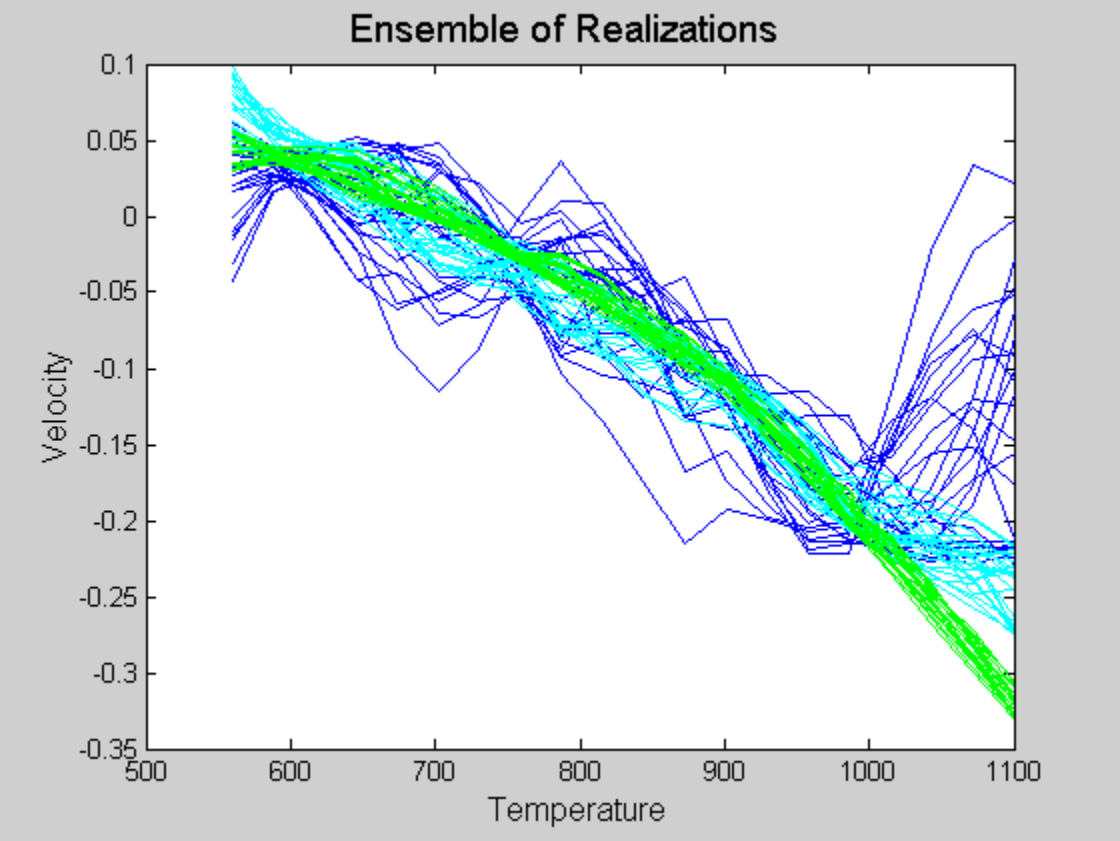

Figure A1. Realizations Approximating the Differences Between Experimental Results and Model Predictions. The green realizations use a quadratic-based random function model; the cyan realizations use a linear-based random function model; and the dark blue use only a random function model.

This Page Intentionally Left Blank

External Distribution

M. A. Adams
Jet Propulsion Laboratory
4800 Oak Grove Drive, MS 97
Pasadena, CA 91109

M. Aivazis
Center for Advanced Computing Research
California Institute of Technology
1200 E. California Blvd./MS 158-79
Pasadena, CA 91125

Charles E. Anderson
Southwest Research Institute
P. O. Drawer 28510
San Antonio, TX 78284-0510

Bilal Ayyub (2)
Department of Civil Engineering
University of Maryland
College Park, MD 20742-3021

Ivo Babuska
TICAM
Mail Code C0200
University of Texas at Austin
Austin, TX 78712-1085

Osman Balci
Department of Computer Science
Virginia Tech
Blacksburg, VA 24061

S. L. Barson
Boeing Company
Rocketdyne Propulsion & Power
MS IB-39
P. O. Box 7922
6633 Canoga Avenue
Canoga Park, CA 91309-7922

Steven Batill (2)
Dept. of Aerospace & Mechanical Engr.
University of Notre Dame
Notre Dame, IN 46556

Ted Belytschko (2)
Department of Mechanical Engineering
Northwestern University
2145 Sheridan Road
Evanston, IL 60208

James Berger
Inst. of Statistics and Decision Science
Duke University
Box 90251
Durham, NC 27708-0251

Jay Boris (2)
Laboratory for Computational Physics and Fluid Dynamics
Naval Research Laboratory
Code 6400
4555 Overlook Ave, SW
Washington, DC 20375-5344

Pavel A. Bouzinov
ADINA R&D, Inc.
71 Elton Avenue
Watertown, MA 02472

John A. Cafeo
General Motors R&D Center
Mail Code 480-106-256
30500 Mound Road
Box 9055
Warren, MI 48090-9055

James C. Cavendish
General Motors R&D Center
Mail Code 480-106-359
30500 Mound Road
Box 9055
Warren, MI 48090-9055

Chun-Hung Chen (2)
Department of Systems Engineering & Operations Research
George Mason University

4400 University Drive, MS 4A6
Fairfax, VA 22030
Wei Chen
Department of Mechanical Engineering
Northwestern University
2145 Sheridan Road, Tech B224
Evanston, IL 60208-3111

Kyeongjae Cho (2)
Dept. of Mechanical Engineering
MC 4040
Stanford University
Stanford, CA 94305-4040

Harry Clark
Rocket Test Operations
AEDC
1103 Avenue B
Arnold AFB, TN 37389-1400

Hugh Coleman
Department of Mechanical &
Aero. Engineering
University of Alabama/Huntsville
Huntsville, AL 35899

Raymond Cosner (2)
Boeing-Phantom Works
MC S106-7126
P. O. Box 516
St. Louis, MO 63166-0516

Thomas A. Cruse
398 Shadow Place
Pagosa Springs, CO 81147-7610

Phillip Cuniff
U.S. Army Soldier Systems Center
Kansas Street
Natick, MA 01750-5019

Department of Energy (4)
Attn: Kevin Greenaugh, NA-115
B. Pate, DD-14
William Reed, DP-141
Jamileh Soudah, NA-114
1000 Independence Ave., SW
Washington, DC 20585

Prof. Urmila Diwekar (2)
University of Illinois at Chicago
Chemical Engineering Dept.
810 S. Clinton St.
209 CHB, M/C 110
Chicago, IL 60607

David Dolling
Department of Aerospace Engineering
& Engineering Mechanics
University of Texas at Austin
Austin, TX 78712-1085

Robert G. Easterling
51 Avenida Del Sol
Cedar Crest, NM 87008

Isaac Elishakoff
Dept. of Mechanical Engineering
Florida Atlantic University
777 Glades Road
Boca Raton, FL 33431-0991

Ashley Emery
Dept. of Mechanical Engineering
Box 352600
University of Washington
Seattle, WA 98195-2600

Scott Ferson
Applied Biomathematics
100 North Country Road
Setauket, New York 11733-1345

Joseph E. Flaherty (2)
Dept. of Computer Science
Rensselaer Polytechnic Institute
Troy, NY 12181

John Fortna
ANSYS, Inc.
275 Technology Drive

Canonsburg, PA 15317

Marc Garbey
Dept. of Computer Science
Univ. of Houston
501 Philipp G. Hoffman Hall
Houston, Texas 77204-3010

Roger Ghanem
Dept. of Civil Engineering
Johns Hopkins University
Baltimore, MD 21218

Mike Giltrud
Defense Threat Reduction Agency
DTRA/CPWS
6801 Telegraph Road
Alexandria, VA 22310-3398

James Glimm (2)
Dept. of Applied Math & Statistics
P138A
State University of New York
Stony Brook, NY 11794-3600

James Gran
SRI International
Poulter Laboratory AH253
333 Ravenswood Avenue
Menlo Park, CA 94025

Bernard Grossman (2)
Dept. of Aerospace &
Ocean Engineering
Mail Stop 0203
215 Randolph Hall
Blacksburg, VA 24061

Sami Habchi
CFD Research Corp.
Cummings Research Park
215 Wynn Drive
Huntsville, AL 35805

Raphael Haftka (2)
Dept. of Aerospace and Mechanical
Engineering and Engr. Science
P. O. Box 116250
University of Florida
Gainesville, FL 32611-6250
Achintya Haldar (2)
Dept. of Civil Engineering
& Engineering Mechanics
University of Arizona
Tucson, AZ 85721

Tim Hasselman
ACTA
2790 Skypark Dr., Suite 310
Torrance, CA 90505-5345

G. L. Havskjold
Boeing - Rocketdyne Propulsion &
Power
MS GB-09
P. O. Box 7922
6633 Canoga Avenue
Canoga Park, CA 91309-7922

George Hazelrigg
Division of Design, Manufacturing
& Innovation
Room 508N
4201 Wilson Blvd.
Arlington, VA 22230

David Higdon
Inst. of Statistics and Decision Science
Duke University
Box 90251
Durham, NC 27708-0251

Richard Hills (2)
Mechanical Engineering Dept.
New Mexico State University
P. O. Box 30001/Dept. 3450
Las Cruces, NM 88003-8001

F. Owen Hoffman (2)
SENES
102 Donner Drive
Oak Ridge, TN 37830

Luc Huyse
Southwest Research Institute
6220 Culebra Road
P. O. Drawer 28510
San Antonio, TX 78284-0510

George Ivy
Northrop Grumman Information Technology
222 West Sixth St.
P.O. Box 471
San Pedro, CA 90733-0471

Rima Izem
Sience and Technology Policy Intern
Board of Mathematical Sciences and their Applications
500 5th Street, NW
Washington, DC 20001

Ralph Jones (2)
Sverdrup Tech. Inc./AEDC Group
1099 Avenue C
Arnold AFB, TN 37389-9013

Leo Kadanoff (2)
Research Institutes Building
University of Chicago
5640 South Ellis Ave.
Chicago, IL 60637

George Karniadakis (2)
Division of Applied Mathematics
Brown University
192 George St., Box F
Providence, RI 02912

Alan Karr
Inst. of Statistics and Decision Science
Duke University
Box 90251
Durham, NC 27708-0251

J. J. Keremes
Boeing Company
Rocketdyne Propulsion & Power
MS AC-15
P. O. Box 7922
6633 Canoga Avenue
Canoga Park, CA 91309-7922

K. D. Kimsey
U.S. Army Research Laboratory
Weapons & Materials Research Directorate
AMSRL-WM-TC 309 120A
Aberdeen Proving Gd, MD 21005-5066

B. A. Kovac
Boeing - Rocketdyne Propulsion & Power
MS AC-15
P. O. Box 7922
6633 Canoga Avenue
Canoga Park, CA 91309-7922

Chris Layne
AEDC
Mail Stop 6200
760 Fourth Street
Arnold AFB, TN 37389-6200

W. K. Liu (2)
Northwestern University
Dept. of Mechanical Engineering
2145 Sheridan Road
Evanston, IL 60108-3111

Robert Lust
General Motors, R&D and Planning
MC 480-106-256
30500 Mound Road
Warren, MI 48090-9055

Sankaran Mahadevan (2)

Dept. of Civil &
Environmental Engineering
Vanderbilt University
Box 6077, Station B
Nashville, TN 37235

Hans Mair
Institute for Defense Analysis
Operational Evaluation Division
4850 Mark Center Drive
Alexandria VA 22311-1882

W. McDonald
NDM Solutions
1420 Aldenham Lane
Reston, VA 20190-3901

Gregory McRae (2)
Dept. of Chemical Engineering
Massachusetts Institute of Technology
Cambridge, MA 02139

Michael Mendenhall (2)
Nielsen Engineering & Research, Inc.
510 Clyde Ave.
Mountain View, CA 94043

Dr. John G. Michopoulos
Naval Research Laboratory,
Special Projects Group, Code 6303
Computational Mutliphysics Systems Lab
Washington DC 20375, USA

Sue Minkoff (2)
Dept. of Mathematics and Statistics
University of Maryland
1000 Hilltop Circle
Baltimore, MD 21250

Max Morris (2)
Department of Statistics
Iowa State University
304A Snedecor-Hall
Ames, IW 50011-1210

R. Namburu
U.S. Army Research Laboratory
AMSRL-CI-H
Aberdeen Proving Gd, MD 21005-5067

NASA/Ames Research Center (2)
Attn: Unmeel Mehta, MS 229-3
David Thompson, MS 269-1
Moffett Field, CA 94035-1000

NASA/Glen Research Center (2)
Attn: John Slater, MS 86-7
Chris Steffen, MS 5-11
21000 Brookpark Road
Cleveland, OH 44135

NASA/Langley Research Center (7)
Attn: Dick DeLoach, MS 236
Michael Hemsch, MS 280
Tianshu Liu, MS 238
Jim Luckring, MS 280
Joe Morrison, MS 128
Ahmed Noor, MS 369
Sharon Padula, MS 159
Hampton, VA 23681-0001

C. Needham
Applied Research Associates, Inc.
4300 San Mateo Blvd., Suite A-220
Albuquerque, NM 87110

A. Needleman
Division of Engineering, Box D
Brown University
Providence, RI 02912

Robert Nelson
Dept. of Aerospace & Mechanical Engr.
University of Notre Dame
Notre Dame, IN 46556

Dick Neumann
8311 SE Millihanna Rd.
Olalla, WA 98359

Efstratios Nikolaidis (2)
MIME Dept.
4035 Nitschke Hall
University of Toledo
Toledo, OH 43606-3390

D. L. O'Connor
Boeing Company
Rocketdyne Propulsion & Power
MS AC-15
P. O. Box 7922
6633 Canoga Avenue
Canoga Park, CA 91309-7922
Tinsley Oden (2)
TICAM
Mail Code C0200
University of Texas at Austin
Austin, TX 78712-1085

Michael Ortiz (2)
Graduate Aeronautical Laboratories
California Institute of Technology
1200 E. California Blvd./MS 105-50
Pasadena, CA 91125

Dale Pace
Applied Physics Laboratory
Johns Hopkins University
111000 Johns Hopkins Road
Laurel, MD 20723-6099

Alex Pang
Computer Science Department
University of California
Santa Cruz, CA 95064

Allan Pifko
2 George Court
Melville, NY 11747

Cary Presser (2)
Process Measurements Div.
National Institute of Standards
and Technology
Bldg. 221, Room B312
Gaithersburg, MD 20899

Thomas A. Pucik
Pucik Consulting Services
13243 Warren Avenue
Los Angles, CA 90066-1750

P. Radovitzky
Graduate Aeronautical Laboratories
California Institute of Technology
1200 E. California Blvd./MS 105-50
Pasadena, CA 91125

W. Rafaniello
DOW Chemical Company
1776 Building
Midland, MI 48674

Chris Rahaim
1793 WestMeade Drive
Chesterfield, MO 63017

Pradeep Raj (2)
Computational Fluid Dynamics
Lockheed Martin Aeronautical Sys.
86 South Cobb Drive
Marietta, GA 30063-0685

J. N. Reddy
Dept. of Mechanical Engineering
Texas A&M University
ENPH Building, Room 210
College Station, TX 77843-3123

John Renaud (2)
Dept. of Aerospace & Mechanical Engr.
University of Notre Dame
Notre Dame, IN 46556

E. Repetto
Graduate Aeronautical Laboratories
California Institute of Technology
1200 E. California Blvd./MS 105-50
Pasadena, CA 91125

Patrick J. Roache
1215 Apache Drive
Socorro, NM 87801

A. J. Rosakis
Graduate Aeronautical Laboratories
California Institute of Technology
1200 E. California Blvd./MS 105-50
Pasadena, CA 91125

Tim Ross (2)
Dept. of Civil Engineering
University of New Mexico
Albuquerque, NM 87131

J. Sacks
Inst. of Statistics and Decision Science
Duke University
Box 90251
Durham, NC 27708-0251

Sunil Saigal (2)
Carnegie Mellon University
Department of Civil and
Environmental Engineering
Pittsburgh, PA 15213

Larry Sanders
DTRA/ASC
8725 John J. Kingman Rd
MS 6201
Ft. Belvoir, VA 22060-6201

Len Schwer
Schwer Engineering & Consulting
6122 Aaron Court
Windsor, CA 95492

Paul Senseny
Factory Mutual Research Corporation
1151 Boston-Providence Turnpike
P.O. Box 9102
Norwood, MA 02062

E. Sevin
Logicon RDA, Inc.
1782 Kenton Circle
Lyndhurst, OH 44124

Mark Shephard (2)
Rensselaer Polytechnic Institute
Scientific Computation Research Center
Troy, NY 12180-3950

Tom I-P. Shih
Dept. of Mechanical Engineering
2452 Engineering Building
East Lansing, MI 48824-1226

T. P. Shivananda
Bldg. SB2/Rm. 1011
TRW/Ballistic Missiles Division
P. O. Box 1310
San Bernardino, CA 92402-1310

Y.-C. Shu
Graduate Aeronautical Laboratories
California Institute of Technology
1200 E. California Blvd./MS 105-50
Pasadena, CA 91125

Don Simons
Northrop Grumman Information Tech.
222 W. Sixth St.
P.O. Box 471
San Pedro, CA 90733-0471

Munir M. Sindir
Boeing - Rocketdyne Propulsion &
Power
MS GB-11

P. O. Box 7922
6633 Canoga Avenue
Canoga Park, CA 91309-7922

Ashok Singhal (2)
CFD Research Corp.
Cummings Research Park
215 Wynn Drive
Huntsville, AL 35805

R. Singleton
Engineering Sciences Directorate
Army Research Office
4300 S. Miami Blvd.
P.O. Box 1221
Research Triangle Park, NC 27709-2211

W. E. Snowden
DARPA
7120 Laketree Drive
Fairfax Station, VA 22039

Bill Spencer (2)
Dept. of Civil Engineering
and Geological Sciences
University of Notre Dame
Notre Dame, IN 46556-0767

Fred Stern
Professor Mechanical Engineering
Iowa Institute of Hydraulic Research
The University of Iowa
Iowa City Iowa 52242

D. E. Stevenson (2)
Computer Science Department
Clemson University
442 Edwards Hall, Box 341906
Clemson, SC 29631-1906

Tim Swafford
Sverdrup Tech. Inc./AEDC Group
1099 Avenue C
Arnold AFB, TN 37389-9013

Kenneth Tatum
Sverdrup Tech. Inc./AEDC Group
740 Fourth Ave.
Arnold AFB, TN 37389-6001

Ben Thacker
Southwest Research Institute
6220 Culebra Road
P. O. Drawer 28510
San Antonio, TX 78284-0510

Fulvio Tonon (2)
Geology and Geophysics Dept.
East Room 719
University of Utah
135 South 1460
Salt Lake City, UT 84112

Robert W. Walters (2)
Aerospace and Ocean Engineering
Virginia Tech
215 Randolph Hall, MS 203
Blacksburg, VA 24061-0203

Leonard Wesley
Intellex Inc.
5932 Killarney Circle
San Jose, CA 95138

Justin Y-T Wu
8540 Colonnade Center Drive, Ste 301
Raleigh, NC 27615

Ren-Jye Yang
Ford Research Laboratory
MD2115-SRL
P.O.Box 2053
Dearborn, MI 4812

Simone Youngblood (2)
DOD/DMSO
Technical Director for VV&A

1901 N. Beauregard St., Suite 504
Alexandria, VA 22311

M. A. Zikry
North Carolina State University
Mechanical & Aerospace Engineering
2412 Broughton Hall, Box 7910
Raleigh, NC 27695

Foreign Distribution

Yakov Ben-Haim (2)
Department of Mechanical Engineering
Technion-Israel Institute of Technology
Haifa 32000
ISRAEL

Gert de Cooman (2)
Universiteit Gent
Onderzoeksgroep, SYSTeMS
Technologiepark - Zwijnaarde 9
9052 Zwijnaarde
BELGIUM

Graham de Vahl Davis
CFD Research Laboratory
University of NSW
Sydney, NSW 2052
AUSTRALIA

Luis Eca (2)
Instituto Superior Tecnico
Department of Mechanical Engineering
Av. Rovisco Pais
1096 Lisboa CODEX
PORTUGAL

Charles Hirsch (2)
Department of Fluid Mechanics
Vrije Universiteit Brussel
Pleinlaan, 2
B-1050 Brussels
BELGIUM

Igor Kozin (2)
Systems Analysis Department
Riso National Laboratory
P. O. Box 49
DK-4000 Roskilde
DENMARK

K. Papoulia
Inst. Eng. Seismology & Earthquake Engineering
P.O. Box 53, Finikas GR-55105
Thessaloniki
GREECE

Dominique Pelletier
Genie Mecanique
Ecole Polytechnique de Montreal
C.P. 6079, Succursale Centre-ville
Montreal, H3C 3A7
CANADA

Vincent Sacksteder
Via Eurialo 28, Int. 13
00181 Rome
Italy

Lev Utkin
Institute of Statistics
Munich University
Ludwigstr. 33
80539, Munich
GERMANY

Malcolm Wallace
Computational Dynamics Ltd.
200 Shepherds Bush Road
London W6 7NY
UNITED KINGDOM

Department of Energy Laboratories

Los Alamos National Laboratory (53)
Mail Station 5000
P.O. Box 1663
Los Alamos, NM 87545
Attn: Peter Adams, MS B220
Mark C. Anderson, MS D411
Robert Benjamin, MS P940
Jane M. Booker, MS P946
Terrence Bott, MS K557
Jerry S. Brock, MS D413
D. Cagliostro, MS F645
Katherine Campbell, MS F600
David L. Crane, MS P946
John F. Davis, MS B295
Helen S. Deaven, MS B295
Barbara DeVolder, MS B259
Scott Doebling, MS P946
S. Eisenhawer, MS K557
Dawn Flicker, MS F664
George T. Gray, MS G755
Ken Hanson, MS B250
Alexandra Heath, MS F663
R. Henninger, MS D413
Brad Holian, MS B268
Kathleen Holian, MS B295
Darryl Holm, MS B284
James Hyman, MS B284
Valen Johnson, MS F600
Cliff Joslyn, MS B265
James Kamm, MS D413
S. Keller-McNulty, MS F600
Joseph Kindel, MS B259
Ken Koch, MS F652
Douglas Kothe, MS B250
Jeanette Lagrange, MS D445
Len Margolin, MS D413
Harry Martz, MS F600
Ryan Maupin, MS T080
Mike McKay, MS F600
Kelly McLenithan, MS F664
Mark P. Miller, MS P946
John D. Morrison, MS F602
Karen I. Pao, MS B256
James Peery, MS F652
M. Peterson-Schnell, MS B295
Douglas Post, MS F661 X-DO
William Rider, MS D413
Tom Seed, MS F663
Kari Sentz, MS B265
David Sharp, MS B213
Richard N. Silver, MS D429
Ronald E. Smith, MS J576
Christine Treml, MS H851
David Tubbs, MS B220
Daniel Weeks, MS B295
Morgan White, MS F663
Alyson G. Wilson, MS F600

Lawrence Livermore National Laboratory
(21)
7000 East Ave.
P.O. Box 808
Livermore, CA 94550

Attn: Thomas F. Adams, MS L-095
Steven Ashby, MS L-561
John Bolstad, MS L-023
Peter N. Brown, MS L-561
T. Scott Carman, MS L-031
R. Christensen, MS L-160
Evi Dube, MS L-095
Henry Hsieh, MS L-229
Richard Klein, MS L-023
Roger Logan, MS L-125
C. F. McMillan, MS L-098
C. Mailhiot, MS L-055
J. F. McEnerney, MS L-023
M. J. Murphy, MS L-282
Daniel Nikkel, MS L-342
Cynthia Nitta, MS L-096
Peter Raboin, MS L-125
Kambiz Salari, MS L-228
Peter Terrill, MS L-125
Charles Tong, MS L-560
Carol Woodward, MS L-561

Argonne National Laboratory (2)
Attn: Paul Hovland
Mike Minkoff
MCS Division
Bldg. 221, Rm. C-236
9700 S. Cass Ave.
Argonne, IL 60439

Sandia Internal Distribution

1 MS 1152 1642 M. L. Kiefer
1 MS 1186 1674 R. J. Lawrence
1 MS 0525 1734 P. V. Plunkett
1 MS 0525 1734 R. B. Heath
1 MS 0525 1734 S. D. Wix
1 MS 0429 2100 J. S. Rottler
1 MS 0429 2100 R. C. Hartwig
1 MS 0447 2111 P. Davis
1 MS 0447 2111 P. D. Hoover
1 MS 0479 2113 J. O. Harrison
1 MS 0487 2115 P. A. Sena
1 MS 0453 2130 H. J. Abeyta
1 MS 0482 2131 K. D. Meeks
1 MS 0482 2131 R. S. Baty
1 MS 0481 2132 M. A. Rosenthal
1 MS 0427 2134 R. A. Paulsen
1 MS 0509 2300 M. W. Callahan
1 MS 0645 2912 D. R. Olson
1 MS 0634 2951 K. V. Chavez
1 MS 0769 5800 D. S. Miyoshi
1 MS 0735 6115 S. C. James
1 MS 0751 6117 L. S. Costin
1 MS 0708 6214 P. S. Veers
1 MS 0490 6252 J. A. Cooper
1 MS 0736 6400 T. E. Blejwas
1 MS 0744 6400 D. A. Powers
1 MS 0747 6410 A. L. Camp
1 MS 0747 6410 G. D. Wyss
1 MS 0748 6413 D. G. Robinson
1 MS 0748 6413 R. D. Waters
1 MS 0576 6536 L. M. Claussen
1 MS 1137 6536 G. K. Froehlich
1 MS 1137 6536 A. L. Hodges
1 MS 1138 6536 M. T. McCornack
1 MS 1137 6536 S. V. Romero
1 MS 1137 6544 S. M. DeLand
1 MS 1137 6545 L. J. Lehoucq
1 MS 1137 6545 G. D. Valdez
1 MS 0720 6804 P. G. Kaplan
1 MS 1395 6820 M. J. Chavez
1 MS 1395 6821 M. K. Knowles
1 MS 1395 6821 J. W. Garner
1 MS 1395 6821 E. R. Giambalvo
1 MS 1395 6821 J. S. Stein
1 MS 0779 6840 M. G. Marietta
1 MS 0779 6840 P. Vaughn
1 MS 0779 6849 J. C. Helton
1 MS 0779 6849 L. C. Sanchez
1 MS 0778 6851 G. E. Barr
1 MS 0778 6851 R. J. MacKinnon
1 MS 0778 6851 P. N. Swift
1 MS 0776 6852 B. W. Arnold
1 MS 0776 6852 T. Hadgu
1 MS 0776 6852 R. P. Rechard
1 MS 9001 8000 J. L. Handrock
1 MS 9007 8200 D. R. Henson
1 MS 9202 8205 R. M. Zurn
1 MS 9005 8240 E. T. Cull, Jr.
1 MS 9051 8351 C. A. Kennedy
1 MS 9405 8700 R. H. Stulen
1 MS 9404 8725 J. R. Garcia
1 MS 9404 8725 W. A. Kawahara
1 MS 9161 8726 E. P. Chen
1 MS 9405 8726 R. E. Jones
1 MS 9161 8726 P. A. Klein
1 MS 9405 8726 R. A. Regueiro
1 MS 9042 8727 J. J. Dike
1 MS 9042 8727 A. R. Ortega
1 MS 9042 8728 C. D. Moen
1 MS 9003 8900 K. E. Washington
1 MS 9003 8940 C. M. Hartwig
1 MS 9217 8962 P. D. Hough
1 MS 9217 8962 K. R. Long
1 MS 9217 8962 M. L. Martinez-Canales
1 MS 9217 8962 J. C. Meza
1 MS 9012 8964 P. E. Nielan
1 MS 0841 9100 T. C. Bickel
1 MS 0841 9100 C. W. Peterson
1 MS 0826 9100 D. K. Gartling
1 MS 0824 9110 A. C. Ratzel
1 MS 0834 9112 M. R. Prairie
1 MS 0834 9112 S. J. Beresh
1 MS 0835 9113 S. N. Kempka
1 MS 0834 9114 J. E. Johannes
1 MS 0834 9114 K. S. Chen
1 MS 0834 9114 R. R. Rao
1 MS 0834 9114 P. R. Schunk

1	MS 0825	9115	B. Hassan	1	MS 0847	9134	S. W. Attaway
1	MS 0825	9115	F. G. Blottner	1	MS 0835	9140	J. M. McGlaun
1	MS 0825	9115	D. W. Kuntz	1	MS 0835	9141	E. A. Boucheron
1	MS 0825	9115	M. A. McWherter-Payne	1	MS 0847	9142	K. F. Alvin
1	MS 0825	9115	J. L. Payne	1	MS 0847	9142	M. L. Blanford
1	MS 0825	9115	D. L. Potter	1	MS 0847	9142	M. W. Heinstein
1	MS 0825	9115	C. J. Roy	1	MS 0847	9142	S. W. Key
1	MS 0825	9115	W. P. Wolfe	1	MS 0847	9142	G. M. Reese
1	MS 0836	9116	E. S. Hertel	1	MS 0826	9143	J. D. Zepper
1	MS 0836	9116	D. Dobranich	1	MS 0827	9143	K. M. Aragon
1	MS 0836	9116	R. E. Hogan	1	MS 0827	9143	H. C. Edwards
1	MS 0836	9116	C. Romero	1	MS 0847	9143	G. D. Sjaardema
1	MS 0836	9117	R. O. Griffith	1	MS 0826	9143	J. R. Stewart
1	MS 0836	9117	R. J. Buss	1	MS 0321	9200	W. J. Camp
1	MS 0847	9120	H. S. Morgan	1	MS 0318	9200	G. S. Davidson
1	MS 0555	9122	M. S. Garrett	1	MS 0847	9211	S. A. Mitchell
1	MS 0893	9123	R. M. Brannon	1	MS 0847	9211	M. S. Eldred
1	MS 0847	9124	J. M. Redmond	1	MS 0847	9211	A. A. Giunta
1	MS 0557	9124	T. G. Carne	1	MS 1110	9211	A. Johnson
1	MS 0847	9124	R. V. Field	5	MS 0819	9211	T. G. Trucano
1	MS 0557	9124	T. Simmermacher	1	MS 0847	9211	B. G. vanBloemenWaanders
1	MS 0553	9124	D. O. Smallwood	1	MS 1176	9211	L. P. Swiler
1	MS 0847	9124	S. F. Wojtkiewicz	1	MS 0316	9212	S. J. Plimpton
1	MS 0557	9125	T. J. Baca	1	MS 1110	9214	D. E. Womble
1	MS 0557	9125	C. C. O'Gorman	1	MS 1110	9214	J. DeLaurentis
1	MS 0847	9126	R. A. May	1	MS 1110	9214	R. B. Lehoucq
1	MS 0847	9126	S. N. Burchett	1	MS 1111	9215	B. A.Hendrickson
1	MS 0847	9126	T. D. Hinnerichs	1	MS 1110	9215	R. Carr
1	MS 0847	9126	K. E. Metzinger	1	MS 1110	9215	S. Y. Chakerian
1	MS 0847	9127	J. Jung	1	MS 1110	9215	W. E. Hart
1	MS 0824	9130	J. L. Moya	1	MS 1110	9215	V. J. Leung
1	MS 1135	9132	L. A. Gritzo	1	MS 1110	9215	C. A. Phillips
1	MS 1135	9132	J. T. Nakos	1	MS 1109	9216	R. J. Pryor
1	MS 1135	9132	S. R. Tieszen	1	MS 0310	9220	R. W. Leland
3	MS 0828	9133	M. Pilch	1	MS 0310	9220	J. A. Ang
1	MS 0828	9133	A. R. Black	1	MS 1110	9223	N. D. Pundit
1	MS 0828	9133	B. F. Blackwell	1	MS 1110	9224	D. W. Doerfler
10	MS 0828	9133	K. J. Dowding	1	MS 0847	9226	P. Knupp
1	MS 0828	9133	W. L. Oberkampf	1	MS 0822	9227	P. D. Heermann
1	MS 0557	9133	T. L. Paez	1	MS 0822	9227	C. F. Diegert
1	MS 0847	9133	J. R. Red-Horse	1	MS 0318	9230	P. Yarrington
1	MS 0828	9133	V. J. Romero	1	MS 0819	9231	R. M. Summers
1	MS 0828	9133	M. P. Sherman	1	MS 0819	9231	K H. Brown
1	MS 0557	9133	A. Urbina	1	MS 0819	9231	S. P. Burns
1	MS 0847	9133	W. R. Witkowski	1	MS 0819	9231	D. E. Carroll
1	MS 1135	9134	S. Heffelfinger	1	MS 0819	9231	M. A. Christon

1	MS 0819	9231	R. R. Drake
1	MS 0819	9231	A. C. Robinson
1	MS 0819	9231	M. K. Wong
1	MS 0820	9232	P. F. Chavez
1	MS 0820	9232	M. E. Kipp
1	MS 0820	9232	S. A. Silling
1	MS 0820	9232	P. A. Taylor
1	MS 0820	9232	J. R. Weatherby
1	MS 0316	9233	S. S. Dosanjh
1	MS 0316	9233	D. R. Gardner
1	MS 0316	9233	S. A. Hutchinson
1	MS 1111	9233	A. G. Salinger
1	MS 1111	9233	J. N. Shadid
1	MS 0316	9235	J. B. Aidun
1	MS 0316	9235	H. P. Hjalmarson
1	MS 0660	9514	M. A. Ellis
1	MS 0660	9519	D. S. Eaton
1	MS 0421	9800	W. Hermina
1	MS 0139	9900	M. O. Vahle
1	MS 0139	9904	R. K. Thomas
1	MS 0139	9905	S. E. Lott
1	MS 0428	12300	D. D. Carlson
1	MS 0428	12301	V. J. Johnson
1	MS 0638	12316	M. A. Blackledge
1	MS 0638	12316	D. L. Knirk
1	MS 0638	12316	D. E. Peercy
1	MS 0829	12323	W. C. Moffatt
1	MS 0829	12323	J. M. Sjulin
10	MS 0829	12323	B. M. Rutherford
1	MS 0829	12323	F. W. Spencer
1	MS 0405	12333	T. R. Jones
1	MS 0405	12333	S. E. Camp
1	MS 0434	12334	R. J. Breeding
1	MS 0830	12335	K. V. Diegert
1	MS 1030	12870	J. G. Miller
1	MS 1170	15310	R. D. Skocypec
1	MS 1176	15312	R. M. Cranwell
1	MS 1176	15312	D. J. Anderson
1	MS 1176	15312	J. E. Campbell
1	MS 1179	15340	J. R. Lee
1	MS 1179	15341	L. Lorence
1	MS 1164	15400	J. L. McDowell
1	MS 1174	15414	W. H. Rutledge
1	MS 9018	8945-1	Central Technical Files
2	MS 0899	9616	Technical Library